Master's thesis

NTNU
Norwegian University of Science and Technology
Faculty of Natural Sciences
Department of Physics

Ulrik Røssevold Flem

Electron-magnon coupling with anisotropic ferromagnets

Master's thesis in Nanotechnology
Supervisor: Asle Sudbø
June 2022

NTNU
Norwegian University of
Science and Technology

Ulrik Røssevold Flem

Electron-magnon coupling with anisotropic ferromagnets

Master's thesis in Nanotechnology
Supervisor: Asle Sudbø
June 2022

Norwegian University of Science and Technology
Faculty of Natural Sciences
Department of Physics

NTNU
Norwegian University of
Science and Technology

Abstract

Heterostructures, where two or more materials are interfacially coupled together, have been gaining interest due to their superconducting properties. In particular, antiferromagnetic insulators (AFMIs) coupled to normal metals (NMs) have been shown to create a stronger magnon mediated electron-electron (e-e) interaction through squeezing of the magnons. The squeezed magnons are achieved by anisotropically coupling the AFMI to the NM. Squeezed magnons are achievable in ferromagnetic insulators (FMIs) through an anisotropic exchange interaction as well. However, the effect of squeezing on the e-e interaction is not known.

This paper studies the e-e interaction in a FMI-NM heterostructure using the BCS model. In particular, the effect of squeezing the FMI-magnons is studied, as well as the effect of adding a second layer to the FMI. It was shown that squeezing of magnons leads to additional spin-triplet interactions that are studied as well. The spin-triplet interaction is found to be 1% the strength of the spin-singlet interaction, making them negligable as contributors to the superconductivity of the heterostructure. It was shown that adding a second layer to the FMI reduces the strength of the interactions, and that a stronger coupling between the two FMI layers further weakens the interactions. When varying the amount of anisotropy in the system, thus varying the amount of squeezing, it was shown that the spin-triplet interaction grew in strength with more anisotropy. However, the spin-singlet interaction is affected by the total amount of exchange interaction rather than the amount of anisotropy. Interactions scattering the electrons into the first and fourth quadrant of the Fermi surface increased in strength with increasing exchange interaction, while it decreased in strength when scattering into the second and third quadrants of the Fermi surface. This effect was the same for both one and two layers of the FMI.

Contents

1 Introduction

Superconductivity is a material phase where electrons pair together to form two-particle states, called Cooper pairs, such that the material resistivity falls to zero [1]. This has obvious uses in the real world, as about 6% of electricity is lost to heat during transmission [2]. Superconducting powerlines would put this loss to zero, reducing energy cost and positively impacting the environment through less energy production. Another important aspect is what is known as the Meissner effect , where a superconductor expels all magnetic fields [3], allowing for for example magnetic levitation, which has wide uses in high speed transportation due to the removal of friction [4]. Furthermore, superconducting magnets are some of the strongest known magnets [5], with uses in for example magnetic imaging, like MRI/NMR [6][7], or particle accelerators, like the large hadron collider[8]. However, superconductivity only appears below a certain temperature, called the critical temperature [1], T_c, which is typically at least 100 degrees celsius below room temperature [9]. Due to the temperature dependence, superconducting materials have yet to see large scale commercial use, as the cost of cooling the superconductor outweighs the cost of the additional energy production. However, with the issues of an emerging climate crisis and an increasing energy need, room-temperature superconductors may be required as a part of the solution.

The phenomenon of superconductivity was first discovered in 1911 by Heike Kamerlingh Onnes who was studying the resistivity of ultrapure Mercury at low temperatures [10], but another 46 years would pass before it was possible to describe what was going on. As it turns out, superconductivity is a purely quantum mechanical phenomenon, but quantum mechanics weren't formulated until 1926 [11]. Moreover, completely new ideas had to be formulated before a theory could be put together. A big clue came when it was discovered that the critical temperature varied with varying isotope mass of the material [12], implying that lattice vibrations (phonons) were involved. In 1957, Bardeen, Cooper and Schrieffer published the BCS theory of superconductivity[13] where they proposed that electrons could form pairs by interacting with a phonon coupling them together. However, when reviewing the theory in later times, it became clear that phonons weren't what was required. Instead, only an attractive interaction to couple the electrons is required. These interactions can be mediated by more exotic particles, like magnons [14][15][16], excitons [17][18] and plasmons [19][20].

Historically, superconductors were thought to only be metallic materials. However, a new type of superconductor was discovered in 1986 by Bednorz and Müller [21] where the critical temperature was higher than previously thought possible. This was the beginning of high-temperature superconductors. The material was a copper oxide, and with this discovery, a family of copper oxide superconductors (cuprates), and later a family of iron-based superconductors [22], were discovered. These, together with some other materials, are known as unconventional superconductors, as the BCS theory fails to provide an explanation for how and why these materials are superconducting. A theory was proposed by Anderson and Baskaran in 1987, called resonating valence bond (RVB) theory [23], focusing on explaining the cuprates, but it is still insufficient as a complete theory for unconventional superconductors.

In common for the cuprates and iron-based superconductors is that they are layered structures, where only specific layers are conducting, while the others serve as charge reservoirs [24]. Due to the layered nature of these materials, it is natural to consider a wider range of layered materials to get a better understanding of the underlying physics. A lot of work has recently been published on heterostructures, where two or more materials are interfacially coupled together, studying their superconducting properties [25]–[31], as well as other properties like spin pumping [32][33], spin currents [34][35] and proximity effetcs [36][37]. Such heterostructures include ferromagnetic insultaors (FMIs) coupled to normal metals (NMs) [38], antiferromagnetic insulators (AFMIs) coupled to NMs [39], topological insulators (TIs) coupled to NMs [40][41] and semiconductors coupled to conventional superconductors [31]. In particular, AFMIs coupled to NMs have shown potential by being able to form stronger magnon-electron couplings due to squeezing of the magnons [42]. Magnon squeezing is an effect where an anisotropic coupling to the NM in AFMIs lead to significantly enhanced attractive electron-electron (e-e) interactions in the heterostructure. Squeezed magnons have also been reported in FMIs through an anisotropic exchange interaction [43], though its effect on the e-e interaction in a FMI-NM heterostructure has not yet been studied.

In most of the superconducting materials mentioned, the Cooper pairs have opposite spins, meaning they are in a spin-singlet state. However, spin-triplet superconductivity, where the two electrons have equal spins, has also been reported [44]–[47]. In particular, it has been found in heavy fermion systems [48], which is another class of unconventional superconductors where the effective masses of the conducting electrons are much larger than the electronic mass [49].

Studying the unconventional superconductors is important not only to understand the underlying physics, but also to understand how the parameters of different materials affect their superconductivity. With the goal of engineering commercial room-temperature superconductors, understanding the mechanisms for it to form Cooper pairs, and the effect of material parameters is crucial. The goal of this paper is thus to contribute to the research and common understanding of superconductivity. In particular, this paper studies the e-e interactions in a FMI-NM heterostructure using the BCS theory, and how they are affected by squeezing the magnons, as well as the effect of adding a second layer to the FMI. The goal is to compare the interaction strengths to the unsqueezed monolayer interaction strength.

To achieve this, the relevant theory is presented in section 2, the model for the FMI-NM heterostructure is derived in section 3, and the e-e interactions are derived in section 4. The interactions are plotted, compared and analysed in sections 5 and 6.

2 Theory

The theory section briefly describes the Bogoliubov transformation and Schrieffer-Wolff transformation, which are needed to rewrite the system Hamiltonian. In addition, it covers the basics of the BCS theory for superconductivity. First of all, however, the conventions used must be mentioned.

2.1 Conventions

In this paper, vectors will be denoted with arrows as $\vec{x}$, while its adjoint will be denoted $\vec{x}^\dagger$. Matrices will be denoted as M. Correspondingly, M^T will be the transpose, M^* will be the complex conjugate, and $M^\dagger = (M^T)^*$ will be the adjoint matrix. The $n \times n$ identity matrix will be denoted I_n. The Pauli matrices will be denoted by $\vec{\sigma}^T = \begin{bmatrix}\sigma_x & \sigma_y & \sigma_z\end{bmatrix}$, where the matrices are defined in the standard way as

$$\sigma_x = \begin{bmatrix}0 & 1\\ 1 & 0\end{bmatrix}, \sigma_y = \begin{bmatrix}0 & -i\\ i & 0\end{bmatrix} \text{ and } \sigma_z = \begin{bmatrix}1 & 0\\ 0 & -1\end{bmatrix},$$

with $i = \sqrt{-1}$ being the imaginary unit.

For simplicity of notation, summing over a quantity, e.g. λ, will always be noted as $\sum_\lambda$ whether λ is a discrete or continuous quantity. Wave vectors $\vec{k}$ and $\vec{q}$ will be written as simply k and q when used as indices or summation variables. Every sum of the type $\sum_q$ and $\sum_k$ means integrating over every $\vec{q}$ or $\vec{k}$ in the first Brillouin zone (1BZ).

In this paper, the reduced Planck's constant $\hbar = \frac{h}{2\pi}$ is set to unity.

2.2 Bogoliubov transformation

The Bogoliubov transformation is a diagonalization of the Hamiltonian, where the transformation works by defining new operators which are linear combinations of the original operators. Moreover, the new operators satisfy the same commutation relation as the original operators. In this paper, only bosonic operators are transformed, so only the bosonic transformation is presented. The theory presented is based in its entirety on work by Tsallis, given in [50]. For further reading on the bosonic Bogoliubov transformation, see also [51].

2.2.1 Deriving the transformation

Assume the Hamiltonian consists of bosonic operators $(a_1, a_2, ..., a_n)$ as well as the adjoint operators $(a_1^\dagger, a_2^\dagger, ..., a_n^\dagger)$ paired up in some way. Define the vector of operators

$$\vec{A}^T = \begin{bmatrix} a_1, & a_2, & ... & a_n, & a_1^\dagger, & ... & a_n^\dagger \end{bmatrix}, \tag{1}$$

such that the Hamiltonian can be written in the form

$$H = \vec{A}^\dagger M \vec{A}, \tag{2}$$

where M is a Hermitian matrix. Then, since the operators are bosonic, the vectors satisfy the bosonic commutation relation

$$\vec{A} \otimes \vec{A}^\dagger - \left((\vec{A}^\dagger)^T \otimes \vec{A}^T\right)^T = J, \tag{3}$$

where $J = \begin{bmatrix} I_n & 0 \\ 0 & -I_n \end{bmatrix}$ and $\otimes$ is the tensor product. Note that J is its own inverse, such that $J^2 = I_{2n}$.

The transformation consists of finding matrices T and D such that D is a diagonal matrix and

$$M = TDT^\dagger. \tag{4}$$

Then

$$H = \vec{A}^\dagger M \vec{A} = \vec{A}^\dagger (TDT^\dagger)\vec{A} = \left(\vec{A}^\dagger T\right) D \left(T^\dagger \vec{A}\right). \tag{5}$$

Thus, $\vec{B} = T^\dagger \vec{A}$ and $\vec{B}^\dagger = \vec{A}^\dagger T$ define a vector of new bosonic operators and its adjoint, such that the new operators are linear combinations of the original operators. Denote these by

$$\vec{B} = \begin{bmatrix} b_1, & b_2, & ... & b_n, & b_1^\dagger, & ... & b_n^\dagger \end{bmatrix}. \tag{6}$$

For the new operators to be bosonic, they must satisfy equation 3 as well. Inserting the definitons of the transformed operators, one finds

$$\begin{gathered} \vec{B} \otimes \vec{B}^\dagger - ((\vec{B}^\dagger)^T \otimes \vec{B}^T)^T = J \\ T^\dagger \vec{A} \otimes \vec{A}^\dagger T - (T^T(\vec{A}^\dagger)^T \otimes \vec{A}^T T^*)^T = J \\ T^\dagger \vec{A} \otimes \vec{A}^\dagger T - T^\dagger((\vec{A}^\dagger)^T \otimes \vec{A}^T)^T T = J \\ T^\dagger(\vec{A} \otimes \vec{A}^\dagger - ((\vec{A}^\dagger)^T \otimes \vec{A}^T)^T)T = J \\ T^\dagger J T = J. \end{gathered}$$

Rewriting the final equality we find that T must satisfy the symplectic relationship

$$T^\dagger = JT^{-1}J. \tag{7}$$

Thus $\vec{B} = JT^{-1}J\vec{A}$. In terms of the column vectors of T, $\vec{v_i}$, the symplectic relationship can also be written as

$$\vec{v_i}^\dagger J \vec{v_j} = J_{ij} = \begin{cases} \delta_{ij}, & i \leq n \\ -\delta_{ij}, & i \geq n+1 \end{cases} \tag{8}$$

which is useful for determining the matrix T. Let vectors satisfying equation 8 be called Bogoliubov orthonormal.

2.2.2 Determining D and T

To find an expression of D in terms of T, notice that

$$\begin{gathered} H = \vec{A}^\dagger M \vec{A} \\ = \vec{A}^\dagger (TT^{-1}) M (J(T(JJ)T^{-1})J)\vec{A} \\ = (\vec{A}^\dagger T)(T^{-1}MJTJ)(JT^{-1}J\vec{A}) \\ = \vec{B}^\dagger \underbrace{T^{-1}MJTJ}_{D} \vec{B}. \end{gathered}$$

Thus

$$D = T^{-1}MJTJ, \tag{9}$$

where solving for MJ gives

$$MJ = T(DJ)T^{-1}. \tag{10}$$

Hence T and DJ makes up a diagonalization of the matrix MJ. DJ contain its eigenvalues and T contains its corresponding eigenvectors.

It can be shown that the eigenvalues of MJ come in pairs of positive and negative. Denote them by $\lambda_{i\pm} = \pm\lambda_i$ for $1 \leq i \leq n$. As for their ordering, let λ_{i+} be the first n eigenvalues, and λ_{i-} be the last n eigenvalues. This guarantees that the eigenvectors are real. Since the eigenvalue matrix is $DJ = diag(\lambda_1, ..., \lambda_n, -\lambda_1, ..., -\lambda_n)$, $D = (DJ)J = diag(\lambda_1, \lambda_2, ..., \lambda_n, \lambda_1, ..., \lambda_n)$ will have all positive elements. Inserting this into the Hamiltonian one gets

$$\begin{aligned} H &= \vec{B}^\dagger D\vec{B} \\ &= \sum_{i=1}^{n} \left(\lambda_i b_i^\dagger b_i + \lambda_i b_i b_i^\dagger\right) \\ &= \sum_{i=1}^{n} \left(\lambda_i b_i^\dagger b_i + \lambda_i (b_i^\dagger b_i + 1)\right) \\ H &= \sum_{i=1}^{n} 2\lambda_i \big(b_i^\dagger b_i + \frac{1}{2}\big), \end{aligned} \tag{11}$$

showing that the Hamiltonian is diagonalized.

T is the eigenvector matrix of MJ. However, the eigenvectors are not generally guaranteed to be Bogoliubov orthonormal, meaning T is not guaranteed to be symplectic. Let $l_i = \sqrt{\vec{v}_i^\dagger J \vec{v}_i}$ be the Bogoliubov length of vector $\vec{v}_i$. Then

$$\vec{x}_i = \frac{1}{l_i}\vec{v}_i \tag{12}$$

constitutes a set of Bogoliubov orthonormal eigenvectors of MJ. Hence

$$T = \begin{bmatrix} \vec{x}_1 & \vec{x}_2 & ... & \vec{x}_{2n} \end{bmatrix}. \tag{13}$$

is symplectic, and $\vec{B} = JT^{-1}J\vec{A}$ is guaranteed to contain bosonic operators.

2.3 Schrieffer-Wolff transformation

The Schrieffer-Wolff (SW) transformation is a unitary transformation of the system Hamiltonian. The transformation perturbatively diagonalizes the Hamiltonian via a perturbation series. The theory presented is based on the original work by Schrieffer and Wolff [52], and only contains the theory required to derive the e-e interactions. For a more thorough and theoretical overview of the SW transformation, see [53].

2.3.1 Deriving the transformation

Suppose the system Hamiltonian can be written in the form $H = H_0 + H_1$, where H_0 is a Hamiltonian with a known complete set of eigenstates $\{|m\rangle\}_{m=1,2,...}$ and corresponding eigenvalues E_m, and H_1 is a perturbation satisfying $\langle m|H_1|m\rangle = 0$ for all m. Note that such a system can always be achieved by including the diagonal elements, H_1^{diag}, of H_1 into H_0. Redefine $H_0' = H_0 + H_1^{diag}$, $H_1' = H_1 - H_1^{diag}$, $E_m' = E_m + \langle m|H_1|m\rangle$, such that $H = H_0' + H_1'$. Assume therefore that $\langle m|H_1|m\rangle = 0$ for all m.

Let S be the generator for the transformation. If H_1 is small, then so will S be too. The transformation is then

$$H' = e^{-S}He^{S}, \tag{14}$$

where a perturbation series can be achieved by Taylor expanding the exponentials. The derivation of the transformed Hamiltonian up to second order in interactions is done in appendix A, and the result is

$$H' = H_0 - \frac{1}{2}[S, H_1], \tag{15}$$

where it is required that $[H_0, S] = -H_1$.

2.3.2 Determining the generator S

Achieving the above expression requires S to satisfy $[H_0, S] = -H_1$. To guarantee this, let S have the same operator structure as H_1. In particular, suppose

$$H_1 = \sum_i C_i a_i A_i, \tag{16}$$

where a_i is some combination of bosonic creation and annihilation operators, A_i is some combination of fermionic creation and annihilation operators, and C_i is the coefficient for that particular combination. Then S is chosen such that

$$S = \sum_i X_i a_i A_i, \tag{17}$$

where a_i's and A_i's are the same as for H_1 and X_i's need to be determined.

2.3.3 Determining the coefficients of S

Suppose $|m\rangle$ and $|n\rangle$ are orthonormal eigenstates of H_0. Then by the definition of S, one has

$$\begin{aligned}
\langle n|[H_0, S]|m\rangle &= \langle n| - H_1|m\rangle \\
\langle n|H_0 S - S H_0|m\rangle &= -\langle n|H_1|m\rangle \\
E_n\langle n|S|m\rangle - \langle n|S|m\rangle E_m &= -\langle n|H_1|m\rangle \\
\langle n|S|m\rangle &= \frac{\langle n|H_1|m\rangle}{E_m - E_n} \\
\sum_i \langle n|X_i a_i A_i|m\rangle &= \sum_i \frac{\langle n|C_i a_i A_i|m\rangle}{E_m - E_n}
\end{aligned} \tag{18}$$

Solving this equation for X_i term by term, the k'th coefficient can be found as

$$\begin{aligned}
\langle n|X_k a_k A_k|m\rangle &= \frac{\langle n|C_k a_k A_k|m\rangle}{E_m - E_n} \\
X_k\langle n|a_k A_k|m\rangle &= \frac{C_k}{E_m - E_n}\langle n|a_k A_k|m\rangle \\
X_k &= \frac{C_k}{E_m - E_n}
\end{aligned} \tag{19}$$

Furthermore, the energies can be determined by noticing that by the orthonormality of the eigenstates, equation 18 is nonzero only if $a_i A_i|m\rangle = |n\rangle$. Since $|m\rangle$ and $|n\rangle$ are many particle states, they can be denoted by the number of particles in each single particle state. In particular $|n\rangle = |n_{\lambda_1}, n_{\lambda_2}, ..., n_{\lambda_p}\rangle$ for p particles in states λ_j. By the orthonormality, $|m\rangle$ must contain one particle in every state that gets annihilated by $a_i A_i$, while $|n\rangle$ must contain a particle in every state that gets created by $a_i A_i$. The many particle energy can then be found as a sum of the energies of the single particle states multiplied by the number of particles in that state. Hence,

$$E_n = \sum_{j=1}^{p} n_{\lambda_j} \cdot \varepsilon_{\lambda_j}, \tag{20}$$

where ε_{λ_j} is the energy of single particle state λ_j.

2.4 BCS theory

The Bardeen-Cooper-Schrieffer (BCS) theory is a microscopic theory of superconductivity that describes the interaction between a pair of electrons when an attractive interaction is stronger than the repulsive Coulomb interaction between them. The section is based on the original 1957 paper by Bardeen, Cooper and Schrieffer [13], as well as Cooper's 1956 paper on the Cooper problem [54].

2.4.1 The Cooper problem

Consider a non-interacting Fermi sea and two additional electrons in states $|\vec{k},\uparrow\rangle$ and $|-\vec{k},\downarrow\rangle$ which only interact with each other and not the Fermi sea. The two electrons can be put in a two-particle state which will be denoted $|\vec{k}\uparrow,-\vec{k}\downarrow\rangle$. After their interaction, assume they scatter into the state $|\vec{k'}\downarrow,-\vec{k'}\uparrow\rangle$. Denote this interaction by V and assume it is only present in a thin shell of width ω_0 around the Fermi surface. In this thin shell, the attractive interaction is stronger than the Coulomb interaction. Denoting the two-particle energy by E, it can be shown that $2\varepsilon_F - E \geq 0$, where ε_F is the Fermi energy. This means the two-particle state lies within the Fermi sea, which seemingly violates the Pauli principle. The two electrons can therefore not be seen as fermions. Instead, consider them as a single two-particle state with creation and annihilation operators

$$\begin{aligned} b_k^\dagger &= c_{k\uparrow}^\dagger c_{-k,\downarrow}^\dagger \\ b_{k'} &= c_{k'\downarrow} c_{-k',\uparrow}, \end{aligned} \tag{21}$$

called a Cooper pair. A Cooper pair is neither a fermion nor a boson, as the operators do not satisfy neither the fermionic nor the bosonic commutation relation. In second quantized form, the Hamiltonian for these two particles looks like

$$H = \varepsilon_{k\uparrow} + \varepsilon_{k\downarrow} + V b_k^\dagger b_{k'} \tag{22}$$

2.4.2 The BCS-model

The BCS theory generalize the Cooper problem to a material containing several electrons in a thin energy shell ω_0 around the Fermi surface. In general, a pair of electrons in a two-particle state $|\vec{k}\sigma,\vec{k'}\sigma'\rangle$ interacting via an interaction V_{eff}, are scattered into state $|\vec{k}+\vec{q},\sigma;\vec{k'}-\vec{q},\sigma'\rangle$. The second-quantized Hamiltonian for the interaction can then be written as

$$H = \sum_{k,\sigma} \varepsilon_{k\sigma} c_{k\sigma}^\dagger c_{k\sigma} + \sum_{k,k',q,\sigma,\sigma'} V_{eff} c_{k+q,\sigma}^\dagger c_{k'-q,\sigma'}^\dagger c_{k'\sigma'} c_{k\sigma}, \tag{23}$$

which is a generalization of equation 22 to multiple electrons. In general, it cannot be guaranteed that $\vec{k}+\vec{q}$ and $\vec{k'}-\vec{q}$ lie within the thin shell around the Fermi surface, so taking inspiration from the Cooper problem, let $\vec{k'} = -\vec{k}$ and $\sigma' = \sigma$, such that

$$H = \sum_{k,\sigma} \varepsilon_{k\sigma} c_{k\sigma}^\dagger c_{k\sigma} + \sum_{k,q,\sigma} V_{eff} c_{k+q,\sigma}^\dagger c_{-k-q,-\sigma}^\dagger c_{-k,-\sigma} c_{k\sigma} \tag{24}$$

and demand that $\vec{q} = \vec{k'} - \vec{k}$. Exchanging $\vec{k}$ and $\vec{k'}$, one achieves the BCS-model of superconductivity

$$H = \sum_{k,\sigma} \varepsilon_{k\sigma} c_{k\sigma}^\dagger c_{k\sigma} - \sum_{k,k'} V_{kk'} c_{k\uparrow}^\dagger c_{-k\downarrow}^\dagger c_{-k',\downarrow} c_{k'\uparrow}, \tag{25}$$

with $V_{k,k'} = -\frac{1}{2} V_{eff}$. The specification $\vec{q} = \vec{k'} - \vec{k}$ along with the redefinition of the momentas when going from equation 23 to 25 is known as BCS reduction. This represents a process where a Cooper pair in state $|\vec{k'}\uparrow,-\vec{k'}\downarrow\rangle$ is scattered into state $|\vec{k}\uparrow,-\vec{k}\downarrow\rangle$.

With this model, the strength of $V_{kk'}$ determines the strength of the Cooper pairs. A large $V_{kk'}$ implies that it is more likely for Cooper pairs to form, which is why comparing the strengths of $V_{kk'}$'s gives information about which one has the largest critical temperature.

3 Models

The heterostructure is described by two different models. One for the ferromagnetic insulator, H_{FM}, and one for the normal metal, H_{NM}. In addition, there is a term coupling the two materials, H_c, such that the full system Hamiltonian can be written as $H = H_{FM} + H_{NM} + H_c$. The lattice in this model is a layered square lattice with N total lattice sites in each layer, where the distance between every nearest neighbour lattice site in the plane is set to 1.

3.1 Model of the ferromagnet

The model used for the FMI is a multilayered quasi two-dimensional Heisenberg model with spin-anisotropic exchange and nearest neighbour interactions. Let layer 1 be at the top, and assume there are M total layers. Suppose the FMI is magnetized towards layer 1. Each layer, k, is modelled as

$$H_1^{(k)} = -\sum_{<i,j>} \left[J S_{iz}^k S_{jz}^k + J_x S_{ix}^k S_{jx}^k + J_y S_{iy}^k S_{jy}^k \right], \tag{26}$$

where S_{iq}^k is the spin component in direction q at lattice site i in layer k. Furthermore, it is assumed that $J_x \neq J_y$ and $J > J_x, J_y$. The notation $< i, j >$ means to sum over all nearest neighbours, j, of every lattice site, i.

The interaction between two neighbouring layers k and $k+1$ is modelled by

$$H_2^{k,k+1} = -J_p \sum_i \vec{S}_i^k \cdot \vec{S}_i^{k+1}, \tag{27}$$

where $\vec{S}_i^k$ is the spin vector at site i in layer k, and J_p is the perpendicular interaction coupling the two layers, with $J_p < J$. Note that it is only nearest neighbour interaction, so $\vec{S}_i^k$ is directly above $\vec{S}_i^{k+1}$.

Rewriting the Hamiltonians in terms of the spin-flip operators $S_{i\pm}^k = S_{ix}^k \pm i S_{iy}^k$, one gets

$$H_1^{(k)} = -\sum_{<i,j>} [J S_{iz}^k S_{jz}^k + \frac{1}{2}\overline{J}(S_{i+}^k S_{j-}^k + S_{i-}^k S_{j+}^k) + \frac{1}{2}\Delta J(S_{i+}^k S_{j+}^k + S_{i-}^k S_{j-}^k)], \tag{28}$$

$$H_2^{k,k+1} = -J_p \sum_i \Big[S_{iz}^k S_{iz}^{k+1} + \frac{1}{2}\big(S_{i+}^k S_{i-}^{k+1} + S_{i-}^k S_{i+}^{k+1}\big) \Big], \tag{29}$$

where $2\overline{J} = J_x + J_y$ and $2\Delta J = J_x - J_y$. Furthermore, let the operators $(a_i^k)^\dagger$ and a_i^k be the spin fluctuation creation and annihilation operators respectively for the spin at lattice site i in layer k. The Holstein-Primakoff transformation then reads as [55]

$$\begin{aligned} S_{iz}^k &= S - (a_i^k)^\dagger a_i^k, \\ S_{i+}^k &= \sqrt{2S} a_i^k, \\ S_{i-}^k &= \sqrt{2S} (a_i^k)^\dagger. \end{aligned} \tag{30}$$

In addition, the inverse Fourier transforms of the lattice fluctuation operators are given by the formulas

$$\begin{aligned} a_i^k &= \frac{1}{\sqrt{N}} \sum_q a_q^k e^{i\vec{r}_i \cdot \vec{q}}, \\ (a_i^k)^\dagger &= \frac{1}{\sqrt{N}} \sum_q (a_q^k)^\dagger e^{-i\vec{r}_i \cdot \vec{q}}, \end{aligned} \tag{31}$$

where $(a_q^k)^\dagger$ and a_q^k are the creation and annihilation operators for magnons with momentum $\vec{q}$ in layer k. Inserting both the Holstein-Primakoff transformation and the inverse Fourier transforms,

the Hamiltonians become

$$H_1^{(k)} = -JNzS^2 + \sum_q \Big[\big(JSz - \overline{J}S\gamma(\vec{q})\big)\big((a_q^k)^\dagger a_q^k + (a_{-q}^k)^\dagger a_{-q}^k\big) \\ -\Delta JS\gamma(\vec{q})\big((a_q^k)^\dagger (a_{-q}^k)^\dagger + a_q^k a_{-q}^k\big)\Big], \tag{32}$$

and

$$H_2^{k,k+1} = -J_pNS^2 + J_pS\sum_q \Big[(a_q^k)^\dagger a_q^k + (a_q^{k+1})^\dagger a_q^{k+1}\Big] \\ -J_pS\sum_q \Big[(a_q^{k+1})^\dagger a_q^k + (a_q^k)^\dagger a_q^{k+1}\Big], \tag{33}$$

where $\gamma(\vec{q}) = \sum_\delta e^{i\vec{\delta}\cdot\vec{q}}$ and $\vec{\delta}$ are the vectors connecting lattice site i to its neighbours. Finally, define the values

$$C_q = JSz - \overline{J}S\gamma(\vec{q}), \tag{34}$$

$$D_q = -\Delta JS\gamma(\vec{q}), \tag{35}$$

$$\Delta = \frac{1}{2}J_pS \tag{36}$$

and sum over all layers to get

$$H_{FM} = \sum_{k=1}^{M} H_1^{(k)} + \sum_{k=1}^{M-1} H_2^{k,k+1}$$

$$= E_0 + \sum_q \Bigg\{ \Big[C_q + \Delta\Big]\Big((a_q^1)^\dagger a_q^1 + (a_{-q}^1)^\dagger a_{-q}^1 + (a_q^M)^\dagger a_q^M + (a_{-q}^M)^\dagger a_{-q}^M\Big) \\ + \Big[C_q + 2\Delta\Big]\sum_{k=2}^{M-1}\Big((a_q^k)^\dagger a_q^k + (a_{-q}^k)^\dagger a_{-q}^k\Big) + D_q\sum_{k=1}^{M}\Big(a_q^k a_{-q}^k + (a_q^k)^\dagger (a_{-q}^k)^\dagger\Big) \\ -\Delta\sum_{k=1}^{M-1}\Big((a_q^{k+1})^\dagger a_q^k + (a_q^k)^\dagger a_q^{k+1} + (a_{-q}^{k+1})^\dagger a_{-q}^k + (a_{-q}^k)^\dagger a_{-q}^{k+1}\Big)\Bigg\}, \tag{37}$$

where $E_0 = -JNzS^2M - J_pNS^2(M-1)$.

Simplify the Hamiltonian by writing it in matrix-form. Define the vector of magnon operators and its adjoint as

$$\vec{\phi}^T = \big[a_q^1, \quad \dots \quad a_q^M, \quad (a_{-q}^1)^\dagger, \quad \dots \quad (a_{-q}^M)^\dagger\big]. \tag{38}$$

$$\vec{\phi}^\dagger = \big[(a_q^1)^\dagger, \quad \dots \quad (a_q^M)^\dagger, \quad a_{-q}^1, \quad \dots \quad a_{-q}^M\big]. \tag{39}$$

The Hamiltonian can then be written as

$$H_{FM} = E_0^* + \sum_q \vec{\phi}^\dagger \underbrace{\begin{bmatrix} U & V \\ V & U \end{bmatrix}}_{P} \vec{\phi}, \tag{40}$$

where $E_0^* = E_0 - M\sum_q C_q - 2N(M-1)\Delta$, $V = D_qI_M$ is a diagonal $M \times M$ matrix, and U is a tridiagonal $M \times M$ matrix of the form

$$U = \begin{bmatrix} C_q+\Delta & -\Delta & 0 & \dots & 0 \\ -\Delta & C_q+2\Delta & -\Delta & & \vdots \\ 0 & & \ddots & & 0 \\ \vdots & & & C_q+2\Delta & -\Delta \\ 0 & \dots & 0 & -\Delta & C_q+\Delta \end{bmatrix}, \tag{41}$$

where only U_{11} and U_{MM} are $C_q + \Delta$, while all other diagonal elements are $C_q + 2\Delta$, and the off-diagonal elements are all equal to $-\Delta$. Thus

$$H_{FM} = E_0^* + \sum_q \vec{\phi}^\dagger P\vec{\phi}. \tag{42}$$

3.2 Model of the normal metal

The normal metal is modelled by a monolayer tight binding model with nearest neighbour hopping at half filling. The Hamiltonian is then

$$H_{NM} = -t \sum_{<i,j>,\sigma} c^\dagger_{i\sigma} c_{j\sigma} - \mu \sum_{i,\sigma} c^\dagger_{i\sigma} c_{i\sigma} - h \sum_{i,\sigma} \sigma c^\dagger_{i\sigma} c_{i\sigma}, \tag{43}$$

where t is the energy of the hopping from lattice site i to a nearest neighbour, j, μ is the chemical potential of the electrons, and h is some external magnetic field coupled to the spin, σ, of the electrons. $c^\dagger_{i\sigma}$ and $c_{i\sigma}$ are the creation and annihilation operators of an electron at lattice site i with spin σ.

The inverse Fourier transforms of the electron creation and annihilation operators are given by

$$\begin{aligned} c_{i\sigma} &= \frac{1}{\sqrt{N}} \sum_k c_{k\sigma} e^{i\vec{r}_i \cdot \vec{k}}, \\ c^\dagger_{i\sigma} &= \frac{1}{\sqrt{N}} \sum_k c^\dagger_{k\sigma} e^{-i\vec{r}_i \cdot \vec{k}}, \end{aligned} \tag{44}$$

where $c^\dagger_{k\sigma}$ and $c_{k\sigma}$ are the creation and annihilation operators for electrons with momentum $\vec{k}$ and spin σ. Inserting the inverse Fourier transforms into the equation for H_{NM} one gets

$$H_{NM} = \sum_{k,\sigma} \varepsilon_{k\sigma} c^\dagger_{k\sigma} c_{k\sigma}, \tag{45}$$

where $\varepsilon_{k\sigma} = \underbrace{-t\gamma(\vec{k}) - \mu}_{\varepsilon_k} - \sigma h$.

3.3 Model of the coupling

The coupling between the two layers is modelled by an exchange interaction between the spins of layer 1 of the FMI and the electron spins of the NM. The Hamiltonian is

$$H_c = -J_{sd} \sum_i \vec{S}^1_i \cdot \vec{s}_i, \tag{46}$$

where J_{sd} is the coupling exchange interaction, $\vec{S}^1_i$ is the spin at lattice site i in layer 1 of the ferromagnet, and $\vec{s}_i$ is the electron spin of the electron at lattice site i. The electron spin vector is defined by $\vec{s}_i = c^\dagger_{i\alpha} \vec{\sigma}_{\alpha\beta} c_{i\beta}$, where $\vec{\sigma}$ is the Pauli matrix and a summation over α, β is implicit.

Rewriting the Hamiltonian in terms of the spin flip operators gives

$$H_c = -J_{sd} \sum_{i\sigma} c^\dagger_{i\sigma} c_{i\sigma} - \frac{J_{sd}}{2} \sum_i \left[S^1_{i+} c^\dagger_{i\downarrow} c_{i\uparrow} + S^1_{i-} c^\dagger_{i\uparrow} c_{i\downarrow} \right]. \tag{47}$$

Inserting the Holstein-Primakoff transformation given by equation 30 as well as the inverse Fourier transforms given by equations 31 and 44 gives the full coupling Hamiltonian as

$$\begin{aligned} H_c = -SJ_{sd} \sum_{k,\sigma} \sigma c^\dagger_{k\sigma} c_{k\sigma} - \sqrt{\frac{2S}{N}} J_{sd} \sum_{k,q} \left[a^1_q c^\dagger_{k+q,\downarrow} c_{k\uparrow} + (a^1_{-q})^\dagger_{k+q,\uparrow} c_{k\downarrow} \right] \\ + \frac{2J_{sd}}{N} \sum_{k_1,k_2,q,\sigma} (a^1_{k_1})^\dagger a^1_{k_2} c^\dagger_{q+k_2-k_1,\sigma} c_{q,\sigma} \end{aligned} \tag{48}$$

Define $V = J_{sd}\sqrt{2S/N}$ and omit the final term of the Hamiltonian for all future calculations, as it does not contain the interactions that are being studied. The final model for the coupling is then

$$H_c = -SJ_{sd} \sum_{k,\sigma} \sigma c^\dagger_{k\sigma} c_{k\sigma} - V \sum_{k,q} \left[a^1_q c^\dagger_{k+q,\downarrow} c_{k\uparrow} + (a^1_{-q})^\dagger_{k+q,\uparrow} c_{k\downarrow} \right]. \tag{49}$$

The final term of this Hamiltonian is what will be considered the perturbation to the full system Hamiltonian.

3.4 Full system model

Combine the three Hamiltonians given by equations 42, 45 and 49 to get the full system Hamiltonian

$$H = H_{FM} + H_{NM} + H_c$$
$$= E_0^* + \sum_q \vec{\phi}^\dagger P \vec{\phi} + \sum_{k\sigma} \varepsilon_{k\sigma} c_{k\sigma}^\dagger c_{k\sigma} - SJ_{sd} \sum_{k\sigma} \sigma c_{k\sigma}^\dagger c_{k\sigma} - V \sum_{k,q} \left[a_q^1 c_{k+q,\downarrow}^\dagger c_{k\uparrow} + (a_{-q}^1)_{k+q,\uparrow}^\dagger c_{k\downarrow} \right] \quad (50)$$

Redefine the electron energies $\varepsilon_{k\sigma} \to \varepsilon_k - \sigma(h + SJ_{sd})$ to combine sums two and three, to get the full system Hamiltonian

$$H = E_0^* + \sum_q \vec{\phi}^\dagger P \vec{\phi} + \sum_{k\sigma} \varepsilon_{k\sigma} c_{k\sigma}^\dagger c_{k\sigma} - V \sum_{k,q} \left[a_q^1 c_{k+q,\downarrow}^\dagger c_{k\uparrow} + (a_{-q}^1)^\dagger c_{k+q,\uparrow} c_{k\downarrow} \right]. \quad (51)$$

The full system is depicted from the side in figure 1.

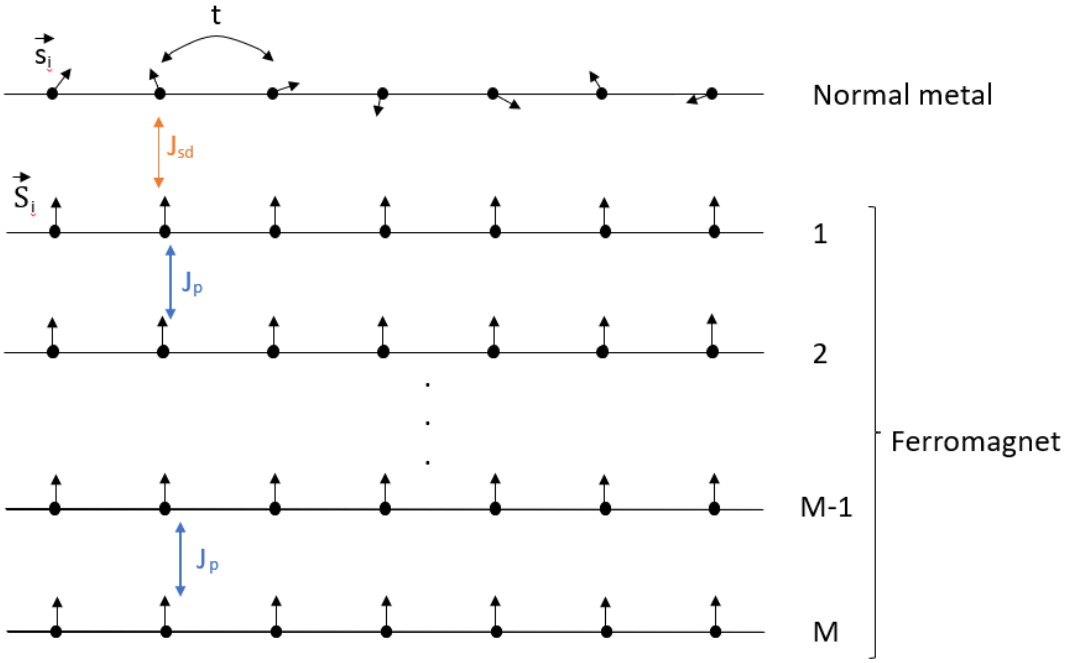

Figure 1: Sideview of the full system. The top layer is the normal metal with unpolarized spins $\vec{s}_i$ and hopping energy t. The normal metal is coupled to the FMI by an interaction J_{sd}. The FMI contains M layers coupled together by an interaction J_p between each layer. All spins $\vec{S}_i$ are polarized towards the normal metal.

4 Deriving the interactions

With the relevant theory and the system Hamiltonian covered, the effective electron-electron interactions can be derived. This chapter first derives the interactions for the monolayer FMI model, and then derives the interactions for the two-layer FMI model. In addition, similarities between the two models are noted during the derivation of the two-layer FMI interactions. In this section, to derive the interactions, the FMI Hamiltonian is Bogoliubov transformed, the full system Hamiltonian is SW transformed in terms of the perturbation, and finally BCS reduced to achieve the effective electron-electron interactions.

4.1 Monolayer FMI model

Consider the full system model with a monolayer of the FMI. In particular, this means that J_p is not present, so it can be set to zero, and $M = 1$.

4.1.1 Bogoliubov transformation of the FMI Hamiltonian

Since there is only one layer, $\Delta = 0$, as this comes from the interlayer coupling. Let a_q^1 be denoted by a_q, as this is the only magnon operator in the model. Then, equation 42 reduces to

$$H_{FM} = E_0^* + \sum_q \begin{bmatrix} a_q^\dagger, & a_{-q} \end{bmatrix} \begin{bmatrix} C_q & D_q \\ D_q & C_q \end{bmatrix} \begin{bmatrix} a_q \\ a_{-q}^\dagger \end{bmatrix}, \tag{52}$$

where $E_0^* = -JNzS^2 - \sum_q C_q$.

Through the Bogoliubov transformation, new operators representing long-lived magnons, A_q and $A_q^\dagger$, are expressed in terms of the operators a_q and $a_q^\dagger$. A detailed walkthrough of the Bogoliubov transformation is presented in appendix B. The new operators are defined by

$$\begin{bmatrix} A_q^\dagger, & A_{-q} \end{bmatrix} = \begin{bmatrix} u_q a_q^\dagger + v_q a_{-q}, & v_q a_q^\dagger + u_q a_{-q} \end{bmatrix}, \tag{53}$$

$$\begin{bmatrix} A_q \\ A_{-q}^\dagger \end{bmatrix} = \begin{bmatrix} u_q a_q + v_q a_{-q}^\dagger \\ v_q a_q + u_q a_{-q}^\dagger \end{bmatrix}, \tag{54}$$

where the coefficients are defined by

$$u_q = \sqrt{\frac{2C_q + \omega_q}{2\omega_q}}, \tag{55}$$

$$v_q = \sqrt{\frac{2C_q - \omega_q}{2\omega_q}}, \tag{56}$$

and

$$\omega_q = 2\sqrt{C_q^2 - D_q^2}. \tag{57}$$

The coefficients can be written in terms of the system parameters as

$$\begin{aligned} u_q^2 &= \frac{1}{2}\left(1 + \frac{Jz - \overline{J}\gamma(q)}{\sqrt{(Jz - J_x\gamma(q))(Jz - J_y\gamma(q))}}\right), \\ v_q^2 &= \frac{1}{2}\left(-1 + \frac{Jz - \overline{J}\gamma(q)}{\sqrt{(Jz - J_x\gamma(q))(Jz - J_y\gamma(q))}}\right), \end{aligned} \tag{58}$$

and satisfy the relationship

$$u_q^2 - v_q^2 = 1. \tag{59}$$

The Bogoliubov transformed FMI Hamiltonian is then

$$H_{FM} = E_0^* + \sum_q \omega_q (A_q^\dagger A_q + \frac{1}{2}), \tag{60}$$

with $E_0^* = -JNzS^2 - \sum_q C_q$ and $\omega_q = 2\sqrt{C_q^2 - D_q^2}$.

4.1.2 The FMI-NM coupling

Consider next the FMI-NM coupling. Before the SW transformation can be performed, the magnon operators a_q and $a_q^\dagger$ must be expressed in terms of the new operators representing long-lived magnons. The Hamiltonian is given by

$$H_c = -V \sum_{k,q} \left[a_q c_{k+q,\downarrow}^\dagger c_{k\uparrow} + a_{-q}^\dagger c_{k+q,\uparrow} c_{k\downarrow} \right]. \tag{61}$$

The inverse Bogoliubov transformation is calculated in appendix B, and found to be

$$\begin{bmatrix} a_q \\ a_{-q}^\dagger \end{bmatrix} = \begin{bmatrix} u_q A_q - v_q A_{-q}^\dagger \\ -v_q A_q + u_q A_{-q}^\dagger \end{bmatrix}, \tag{62}$$

$$\begin{bmatrix} a_q^\dagger & a_{-q} \end{bmatrix} = \begin{bmatrix} u_q A_q^\dagger - v_q A_{-q}, & -v_q A_q^\dagger + u_q A_{-q} \end{bmatrix}. \tag{63}$$

Inserting this into equation 61 we get

$$H_c = -V \sum_{k,q} \Big[u_q A_q c_{k+q,\downarrow}^\dagger c_{k\uparrow} - v_q A_{-q}^\dagger c_{k+q,\downarrow}^\dagger c_{k\uparrow} + u_q A_{-q}^\dagger c_{k+q,\uparrow} c_{k\downarrow} - v_q A_q c_{k+q,\uparrow} c_{k\downarrow} \Big], \tag{64}$$

which will be used as the perturbation for the SW transformation.

4.1.3 SW transformation

After the Bogoliubov transformation, the system Hamiltonian can be written as

$$\begin{aligned} H &= E_0^* + \sum_q \omega_q (A_q^\dagger A_q + \frac{1}{2}) + \sum_{k\sigma} \varepsilon_{k\sigma} c_{k\sigma}^\dagger c_{k\sigma} \\ -V \sum_{k,q} &\Big[u_q A_q c_{k+q,\downarrow}^\dagger c_{k\uparrow} - v_q A_{-q}^\dagger c_{k+q,\downarrow}^\dagger c_{k\uparrow} + u_q A_{-q}^\dagger c_{k+q,\uparrow} c_{k\downarrow} - v_q A_q c_{k+q,\uparrow} c_{k\downarrow} \Big] \end{aligned} \tag{65}$$

This Hamiltonian can now be diagonalized using a SW transformation in accordance with the method presented in section 2.3. The ground state Hamiltonian is

$$H_0 = E_0^* + \sum_q \omega_q (A_q^\dagger A_q + \frac{1}{2}) + \sum_{k\sigma} \varepsilon_{k\sigma} c_{k\sigma}^\dagger c_{k\sigma}, \tag{66}$$

the perturbation is

$$H_1 = H_c = -V \sum_{k,q} \Big[u_q A_q c_{k+q,\downarrow}^\dagger c_{k,\uparrow} + u_q A_{-q}^\dagger c_{k+q,\uparrow}^\dagger c_{k,\downarrow} - v_q A_{-q}^\dagger c_{k+q,\downarrow}^\dagger c_{k,\uparrow} - v_q A_q c_{k+q,\uparrow}^\dagger c_{k,\downarrow} \Big], \tag{67}$$

and as described in section 2.3 the generator for the SW transformation has the same operator structure as H_1, so it becomes

$$S = -V \sum_{k,q} \Big[X_{kq} A_q c_{k+q,\downarrow}^\dagger c_{k\uparrow} + Y_{kq} A_{-q}^\dagger c_{k+q,\uparrow}^\dagger c_{k\downarrow} + Z_{kq} A_{-q}^\dagger c_{k+q,\downarrow}^\dagger c_{k\uparrow} + W_{kq} A_q c_{k+q,\uparrow}^\dagger c_{k\downarrow} \Big], \tag{68}$$

where X_{kq}, Y_{kq}, Z_{kq} and W_{kq} need to be determined. The diagonalized Hamiltonian is then

$$H' = H_0 - \frac{1}{2}[S, H_1]. \tag{69}$$

The coefficients of S are calculated in accordance with the method presented in section 2.3.3 in appendix C, and are shown to be

$$X_{kq} = \frac{u_q}{\varepsilon_{k\uparrow} - \varepsilon_{k+q,\downarrow} + \omega_q}, \tag{70}$$

$$Y_{kq} = \frac{u_q}{\varepsilon_{k,\downarrow} - \varepsilon_{k+q,\uparrow} - \omega_q}, \tag{71}$$

$$Z_{kq} = \frac{v_q}{\varepsilon_{k+q,\downarrow} - \varepsilon_{k\uparrow} + \omega_q}, \tag{72}$$

$$W_{kq} = \frac{v_q}{\varepsilon_{k+q,\uparrow} - \varepsilon_{k\downarrow} - \omega_q}. \tag{73}$$

Furthermore, the commutator $[S, H_1]$ is calculated in appendix D. When calculating it we find

$$-\frac{1}{2}[S,H_1] = -\sum_{k,k',q}\Big[V_{eff}^{opposite}c_{k+q,\downarrow}^{\dagger}c_{k'-q,\uparrow}^{\dagger}c_{k\uparrow}c_{k'\downarrow}+V_{eff}^{up}c_{k+q,\uparrow}^{\dagger}c_{k'-q,\uparrow}^{\dagger}c_{k\downarrow}c_{k'\downarrow}+V_{eff}^{down}c_{k+q,\downarrow}^{\dagger}c_{k'-q,\downarrow}^{\dagger}c_{k\uparrow}c_{k'\uparrow}\Big], \tag{74}$$

where

$$V_{eff}^{opposite} = -\frac{V^2}{2}\big(X_{kq}u_q + Z_{kq}v_q - Y_{k',-q}u_q - W_{k',-q}v_q\big), \tag{75}$$

$$V_{eff}^{up} = -\frac{V^2}{2}\big(Y_{k',-q}v_q + W_{kq}u_q\big), \tag{76}$$

$$V_{eff}^{down} = \frac{V^2}{2}\big(X_{kq}v_q + Z_{k',-q}u_q\big) \tag{77}$$

The diagonalized system Hamiltonian is then

$$H = E_0^* + \sum_q \omega_q(A_q^{\dagger}A_q + \frac{1}{2}) + \sum_{k\sigma}\varepsilon_{k\sigma}c_{k\sigma}^{\dagger}c_{k\sigma}$$
$$-\sum_{k,k',q}\Big[V_{eff}^{opposite}c_{k+q,\downarrow}^{\dagger}c_{k'-q,\uparrow}^{\dagger}c_{k\uparrow}c_{k'\downarrow} + V_{eff}^{up}c_{k+q,\uparrow}^{\dagger}c_{k'-q,\uparrow}^{\dagger}c_{k\downarrow}c_{k'\downarrow} + V_{eff}^{down}c_{k+q,\downarrow}^{\dagger}c_{k'-q,\downarrow}^{\dagger}c_{k\uparrow}c_{k'\uparrow}\Big]. \tag{78}$$

Most noteworthy is the fact that three different spin structures with different electron-electron interactions appear. There is the spin-singlet $|\uparrow,\downarrow\rangle \to |\downarrow,\uparrow\rangle$ interaction that appears in the Cooper problem, but when introducing squeezing, additional spin-triplet interactions $|\uparrow,\uparrow\rangle \to |\downarrow,\downarrow\rangle$ and $|\downarrow,\downarrow\rangle \to |\uparrow,\uparrow\rangle$ appear. Only the spin-singlet interaction is predicted by the BCS-model. The origin of these interactions are discussed in section 6.1.

4.1.4 BCS reduction

To guarantee that the interactions scatter the Cooper pairs onto the region of width ω_0 around the Fermi surface, the interaction term of the system Hamiltonian must be BCS reduced in accordance with section 2.4.2. This means specifying the impulse $\vec{q}$ to scatter $\vec{k}'$ to $\vec{k}$. The procedure consists of redefining the momentas as $\vec{k}' \to -\vec{k}$, setting $\vec{q} = \vec{k}' - \vec{k}$ and finally exchanging $\vec{k}$ and $\vec{k}'$. The interaction term then becomes

$$-\sum_{k,k',q}\Big[V_{kk'}^{opposite}c_{k,\downarrow}^{\dagger}c_{-k,\uparrow}^{\dagger}c_{k'\uparrow}c_{-k',\downarrow} + V_{kk'}^{up}c_{k,\uparrow}^{\dagger}c_{-k,\uparrow}^{\dagger}c_{k'\downarrow}c_{-k',\downarrow} + V_{kk'}^{down}c_{k,\downarrow}^{\dagger}c_{-k,\downarrow}^{\dagger}c_{k'\uparrow}c_{-k',\uparrow}\Big]. \tag{79}$$

The BCS reduction of the interactions are performed in appendix E, with the result being

$$V_{kk'}^{opposite} = \frac{V^2u_{k-k'}^2\tilde{\omega}_{k-k'}^{-}}{(\varepsilon_k-\varepsilon_{k'})^2-(\tilde{\omega}_{k-k'}^{-})^2} + \frac{V^2v_{k-k'}^2\tilde{\omega}_{k-k'}^{+}}{(\varepsilon_k-\varepsilon_{k'})^2-(\tilde{\omega}_{k-k'}^{+})^2}, \tag{80}$$

$$V_{kk'}^{up} = \frac{V^2u_{k-k'}v_{k-k'}\omega_{k-k'}}{\widetilde{\omega}_{k-k'}^{+}\widetilde{\omega}_{k-k'}^{-} + (\varepsilon_k-\varepsilon_{k'})(\widetilde{\omega}_{k-k'}^{+}-\widetilde{\omega}_{k-k'}^{-}) - (\varepsilon_k-\varepsilon_{k'})^2}, \tag{81}$$

$$V_{kk'}^{down} = \frac{V^2u_{k-k'}v_{k-k'}\omega_{k-k'}}{\widetilde{\omega}_{k-k'}^{+}\widetilde{\omega}_{k-k'}^{-} - (\varepsilon_k-\varepsilon_{k'})(\widetilde{\omega}_{k-k'}^{+}-\widetilde{\omega}_{k-k'}^{-}) - (\varepsilon_k-\varepsilon_{k'})^2}, \tag{82}$$

after the coefficients are inserted. In the above expressions, $\varepsilon_{k\sigma}$ has been split into $\varepsilon_{k\sigma} = \underbrace{-t\gamma(\vec{k})-\mu}_{\varepsilon_k} - (h+2SJ_{sd})\sigma$ and $\widetilde{\omega}_q^{\pm} = \omega_q \pm 2(h+SJ_{sd})$.

Note that $V_{kk'}^{up}$ and $V_{kk'}^{down}$ only vary by the sign of the second term in the denominator. Both these terms are proportional to $\varepsilon_k - \varepsilon_{k'}$, which means that for scattering at the Fermi surface, these terms cancel out, such that the interactions are identical.

4.2 Two-layer FMI model

Consider next the model with two layers of the FMI. With two layers, J_p is introduced into the FMI Hamiltonian, and can not be considered zero as in the monolayer model.

4.2.1 Bogoliubov transformation of the FMI Hamiltonian

Let a_q^1 be denoted by a_q and a_q^2 by b_q for simplicity of notation. From equation 42, the two-layer FMI Hamiltonian is

$$H = E_0^* + \sum_q \begin{bmatrix} a_q^\dagger, & b_q^\dagger, & a_{-q} & b_{-q} \end{bmatrix} \begin{bmatrix} C_q + \Delta & -\Delta & D_q & 0 \\ -\Delta & C_q + \Delta & 0 & D_q \\ D_q & 0 & C_q + \Delta & -\Delta \\ 0 & D_q & -\Delta & C_q + \Delta \end{bmatrix} \begin{bmatrix} a_q \\ b_q \\ a_{-q}^\dagger \\ b_{-q}^\dagger \end{bmatrix}, \tag{83}$$

where $E_0^* = -2JNzS^2 - J_pNS^2 - 2\sum_q C_q - 2N\Delta$.

As for the monolayer model, H_{FM} is Bogoliubov transformed to be expressed in terms of operators representing long-lived magnons. Denote the new operators by $A_q^1 = A_q$ and $A_q^2 = B_q$. The Bogoliubov transformation is performed in appendix F. The transformed Hamiltonian is

$$H = E_0^* + \sum_{q,i} \omega_{qi} \big((A_q^i)^\dagger A_q^i + \frac{1}{2} \big), \tag{84}$$

where $i = 1, 2$, and the magnon spectras are given by

$$\omega_{q1} = 2\sqrt{C_q^2 - D_q^2}, \tag{85}$$

$$\omega_{q2} = 2\sqrt{(C_q + 2\Delta)^2 - D_q^2}. \tag{86}$$

The transformed operators are defined in terms of the old operators as

$$\begin{bmatrix} A_q^\dagger \\ B_q^\dagger \\ A_q \\ B_q \end{bmatrix} = \begin{bmatrix} u_{q1} a_q^\dagger + u_{q1} b_q^\dagger + v_{q1} a_{-q} + v_{q1} b_{-q} \\ -u_{q2} a_q^\dagger + u_{q2} b_q^\dagger - v_{q2} a_{-q} + v_{q2} b_{-q} \\ u_{q1} a_q + u_{q1} b_q + v_{q1} a_{-q}^\dagger + v_{q1} b_{-q}^\dagger \\ -u_{q2} a_q + u_{q2} b_q - v_{q2} a_{-q}^\dagger + v_{q2} b_{-q}^\dagger \end{bmatrix}, \tag{87}$$

where the coefficients are defined by

$$u_{q1} = \sqrt{\frac{2C_q + \omega_{q1}}{4\omega_{q1}}}, \tag{88}$$

$$u_{q2} = \sqrt{\frac{2(C_q + 2\Delta) + \omega_{q2}}{4\omega_{q2}}}, \tag{89}$$

$$v_{q1} = \sqrt{\frac{2C_q - \omega_{q1}}{4\omega_{q1}}}, \tag{90}$$

$$v_{q2} = \sqrt{\frac{2(C_q + 2\Delta) - \omega_{q2}}{4\omega_{q2}}}. \tag{91}$$

These coefficients satisfy similar relationships to equation 59 in the monolayer model, namely

$$\begin{aligned} u_{q1}^2 - v_{q1}^2 &= \frac{1}{2}, \\ u_{q2}^2 - v_{q2}^2 &= \frac{1}{2}, \\ (u_{q1}^2 + u_{q2}^2) - (v_{q1}^2 + v_{q2}^2) &= 1. \end{aligned} \tag{92}$$

Moreover, u_{q1} and v_{q1} are related to u_q and v_q in the monolayer model via the relations

$$\begin{aligned} u_{q1} &= \frac{1}{\sqrt{2}} u_q, \\ v_{q1} &= \frac{1}{\sqrt{2}} v_q, \end{aligned} \tag{93}$$

while ω_{q1} is identical to ω_q in the monolayer model. Notably, there is no dependence on J_p. When looking at equation 87, A_q and $A_q^\dagger$ are equally dependent on the a_q and b_q operators, implying that the spins in both layers fluctuate parallel to each other, thus eliminating their interaction with each other. Meanwhile, B_q and $B_q^\dagger$ have opposite signs for their dependence on the a_q and b_q operators, implying that the spin fluctuations in layer 2 are 180° out of phase with the spin fluctuations in layer 1.

4.2.2 The FMI-NM coupling

Consider next the coupling term given by

$$H_c = -V \sum_{k,q} \left[a_q c_{k+q,\downarrow}^\dagger c_{k\uparrow} + a_{-qk+q,\uparrow}^\dagger c_{k\downarrow} \right]. \tag{94}$$

The Hamiltonian must be expressed in terms of the new operators. The inverse Bogoliubov transformation of the magnon operators is calculated in appendix F and is given by

$$\begin{bmatrix} a_q \\ a_{-q}^\dagger \end{bmatrix} = \begin{bmatrix} u_{q1} A_q - u_{q2} B_q - v_{q1} A_{-q}^\dagger + v_{q2} B_{-q}^\dagger \\ -v_{q1} A_q + v_{q2} B_q + u_{q1} A_{-q}^\dagger - u_{q2} B_{-q}^\dagger \end{bmatrix}. \tag{95}$$

To more easily compare the two-layer FMI model to the monolayer model, write this as

$$a_q = \sum_{i=1}^{2} (-1)^{i+1} \left[u_{qi} A_q^i - v_{qi} (A_{-q}^i)^\dagger \right], \tag{96}$$

$$a_{-q}^\dagger = \sum_{i=1}^{2} (-1)^{i+1} \left[-v_{qi} A_q^i + u_{qi} (A_{-q}^i)^\dagger \right], \tag{97}$$

where $A_q^1 = A_q$ and $A_q^2 = B_q$. Inserting them into H_c gives

$$H_c = -V \sum_{k,q,i} (-1)^{i+1} \Big[u_{qi} A_q^i c_{k+q,\downarrow}^\dagger c_{k\uparrow} - v_{qi} (A_{-q}^i)^\dagger c_{k+q,\downarrow}^\dagger c_{k\uparrow} + u_{qi} (A_{-q}^i)^\dagger c_{k+q,\uparrow} c_{k\downarrow} - v_{qi} A_q^i c_{k+q,\uparrow} c_{k\downarrow} \Big], \tag{98}$$

which has the exact same form as H_c in the monolayer model up to the summation over i.

4.2.3 SW transformation

The Bogoliubov transformed system Hamiltonian is

$$\begin{aligned} H = E_0^* + \sum_{k,\sigma} \varepsilon_{k\sigma} c_{k\sigma}^\dagger c_{k\sigma} + \sum_{q,i} \omega_{qi} ((A_q^i)^\dagger A_q^i + \frac{1}{2}) \\ -V \sum_{k,q,i} (-1)^{i+1} \Big[u_{qi} A_q^i c_{k+q,\downarrow}^\dagger c_{k\uparrow} - v_{qi} (A_{-q}^i)^\dagger c_{k+q,\downarrow}^\dagger c_{k\uparrow} + u_{qi} (A_{-q}^i)^\dagger c_{k+q,\uparrow}^\dagger c_{k\downarrow} - v_{qi} A_q^i c_{k+q,\uparrow}^\dagger c_{k\downarrow} \Big], \end{aligned} \tag{99}$$

The Hamiltonian can be diagonalized by the SW transformation as described in section 2.3. The ground state Hamiltonian is

$$H_0 = E_0^* + \sum_{k,\sigma} \varepsilon_{k\sigma} c_{k\sigma}^\dagger c_{k\sigma} + \sum_{q,i} \omega_{qi} ((A_q^i)^\dagger A_q^i + \frac{1}{2}), \tag{100}$$

the perturbation is the interaction term

$$H_1 = H_c = -V\sum_{k,q,i}(-1)^{i+1}\Big[u_{qi}A^i_q c^\dagger_{k+q,\downarrow}c_{k\uparrow} - v_{qi}(A^i_{-q})^\dagger c^\dagger_{k+q,\downarrow}c_{k\uparrow} + u_{qi}(A^i_{-q})^\dagger c^\dagger_{k+q,\uparrow}c_{k\downarrow} - v_{qi}A^i_q c^\dagger_{k+q,\uparrow}c_{k\downarrow}\Big], \tag{101}$$

so the generator of the transformation is

$$S = -V\sum_{k,q,i}(-1)^{i+1}\Big[X^i_{kq}A^i_q c^\dagger_{k+q,\downarrow}c_{k\uparrow} + Y^i_{kq}(A^i_{-q})^\dagger c^\dagger_{k+q,\uparrow}c_{k\downarrow} + Z^i_{kq}(A^i_{-q})^\dagger c^\dagger_{k+q,\downarrow}c_{k\uparrow} + W^i_{kq}A^i_q c^\dagger_{k+q,\uparrow}c_{k\downarrow}\Big], \tag{102}$$

where X^i_{kq}, Y^i_{kq}, Z^i_{kq} and W^i_{kq} must be determined to get the transformed Hamiltonian

$$H' = H_0 - \frac{1}{2}[S, H_1]. \tag{103}$$

The coefficients are calculated in appendix G as described in section 2.3.3. They are

$$X^i_{kq} = \frac{u_{qi}}{\varepsilon_{k\uparrow} - \varepsilon_{k+q,\downarrow} + \omega_{qi}}, \tag{104}$$

$$Y^i_{kq} = \frac{u_{qi}}{\varepsilon_{k\downarrow} - \varepsilon_{k+q,\uparrow} - \omega_{qi}}, \tag{105}$$

$$Z^i_{kq} = \frac{v_{qi}}{\varepsilon_{k+q,\downarrow} - \varepsilon_{k,\uparrow} + \omega_{qi}}, \tag{106}$$

$$W^i_{kq} = \frac{v_{qi}}{\varepsilon_{k+q,\uparrow} - \varepsilon_{k,\downarrow} - \omega_{qi}}, \tag{107}$$

which is the exact same form as the coefficients in the monolayer model.

The commutator is calculated in appendix H and found to be

$$-\frac{1}{2}[S, H_1] = -\sum_{k,k',q}\Big[V^{opposite}_{eff}c^\dagger_{k+q,\downarrow}c^\dagger_{k'-q,\uparrow}c_{k\uparrow}c_{k'\downarrow} + V^{up}_{eff}c^\dagger_{k+q,\uparrow}c^\dagger_{k'-q,\uparrow}c_{k\downarrow}c_{k'\downarrow} + V^{down}_{eff}c^\dagger_{k+q,\downarrow}c^\dagger_{k'-q,\downarrow}c_{k\uparrow}c_{k'\uparrow}\Big], \tag{108}$$

where

$$V^{opposite}_{eff} = -\frac{V^2}{2}\sum_{i=1}^{2}\big(Z^i_{kq}v_{qi} + X^i_{kq}u_{qi} - Y^i_{k',-q}u_{qi} - W_{k',-q}v_{qi}\big), \tag{109}$$

$$V^{up}_{eff} = -\frac{V^2}{2}\sum_{i=1}^{2}\big(W^i_{kq}u_{qi} + Y^i_{k',-q}v_{qi}\big), \tag{110}$$

$$V^{down}_{eff} = \frac{V^2}{2}\sum_{i=1}^{2}\big(X^i_{kq}v_{qi} + Z_{k',-q}u_{qi}\big). \tag{111}$$

The interactions are also identical to the interactions in the monolayer model up to the summation over i. This includes the spin-triplet interactions, which are present in the two-layer model as well. As previously stated, their origin is discussed in section 6.1.

4.2.4 BCS reduction

The interaction term of the Hamiltonian must be BCS reduced to guarantee that the Cooper pairs scatter into the region of width ω_0 around the Fermi surface. In accordance with the procedure presented in section 2.4.2, this consists of redefining the momentas $\vec{k}' \to -\vec{k}$, setting $\vec{q} = \vec{k}' - \vec{k}$ and exchanging all $\vec{k}$ and $\vec{k}'$. Doing so gives the interaction term as

$$-\frac{1}{2}[S, H_1] = -\sum_{k,k',i}\Big[V^{opposite}_{kk'}c^\dagger_{k\downarrow}c^\dagger_{-k,\uparrow}c_{k'\uparrow}c_{-k',\downarrow} + V^{up}_{kk'}c^\dagger_{k\uparrow}c^\dagger_{-k,\uparrow}c_{k'\downarrow}c_{-k',\downarrow} + V^{down}_{kk'}c^\dagger_{k\downarrow}c^\dagger_{-k,\downarrow}c_{k'\uparrow}c_{-k',\uparrow}\Big]. \tag{112}$$

The BCS reduction of the interactions is performed in appendix I and gives

$$V_{kk'}^{opposite} = \sum_{i=1}^{2} \Big(\frac{V^2 u_{k-k',i}^2 \tilde{\omega}_{k-k',i}^-}{(\varepsilon_k - \varepsilon_{k'})^2 - (\tilde{\omega}_{k-k',i}^-)^2} + \frac{V^2 v_{k-k',i}^2 \tilde{\omega}_{k-k',i}^+}{(\varepsilon_k - \varepsilon_{k'})^2 - (\tilde{\omega}_{k-k',i}^+)^2} \Big), \tag{113}$$

$$V_{kk'}^{up} = \sum_{i=1}^{2} \frac{V^2 u_{k-k',i} v_{k-k',i} \omega_{k-k',i}}{\tilde{\omega}_{k-k',i}^+ \tilde{\omega}_{k-k',i}^- + (\tilde{\omega}_{k-k',i}^+ - \tilde{\omega}_{k-k',i})(\varepsilon_k - \varepsilon_{k'}) - (\varepsilon_k - \varepsilon_{k'})^2}, \tag{114}$$

$$V_{kk'}^{down} = \sum_{i=1}^{2} \frac{V^2 u_{k-k',i} v_{k-k',i} \omega_{k-k',i}}{\tilde{\omega}_{k-k',i}^+ \tilde{\omega}_{k-k',i}^- - (\tilde{\omega}_{k-k',i}^+ - \tilde{\omega}_{k-k',i})(\varepsilon_k - \varepsilon_{k'}) - (\varepsilon_k - \varepsilon_{k'})^2}, \tag{115}$$

where $\varepsilon_k = -t\gamma(\vec{k}) - \mu$ and $\tilde{\omega}_{qi}^{\pm} = \omega_{qi} \pm 2(h + SJ_{sd})$. Once again, the expressions are identical to the interactions in the monolayer model up to the summation over i.

5 Calculations and results

With all the effective electron-electron interactions derived, their strength can be calculated. This section first approximates the Fermi surface and describes how the strengths are calculated in section 5.1, and then plots the relevant graphs for the monolayer model in section 5.2, and two-layer model in section 5.3.

5.1 Method of calculations

As stated in section 2.4, the interactions are only valid in a small region around the Fermi surface. To simplify the calculations, the interactions will therefore be calculated only on the Fermi surface. In the model for the normal metal, the Fermi energy is the chemical potential, μ. Since this is included in the expression for $\varepsilon_{k\sigma}$, the Fermi surface is defined by the zero point of the electron energy, given by

$$\varepsilon_{k\sigma} = -t\gamma(\vec{k}) - \mu - \sigma(h + SJ_{sd}) = 0, \tag{116}$$

which gives a spin splitting of the Fermi surface. However, t is the dominant energy term in the model, so the spin-dependence will be neglected for the evaluations of the interactions. As calculated in appendix J, the Fermi surface then becomes

$$\cos(k_x) + \cos(k_y) = -\frac{\mu}{2t}. \tag{117}$$

Since the maximum of $\cos(k_x) + cos(k_y)$ is 2, and the metal is at half filling, let the Fermi energy be $\mu = -2t$, such that the Fermi surface becomes

$$\cos(k_x) + \cos(k_y) = 1. \tag{118}$$

To simplify the calculations, approximate the Fermi surface as a circle. The rightmost point on the Fermi surface is at the point $(k_x, k_y) = (\frac{\pi}{2}, 0)$, so let the radius be $\frac{\pi}{2}$. The approximated Fermi surface then becomes

$$k_x^2 + k_y^2 = \frac{\pi^2}{4}. \tag{119}$$

The original Fermi surface as well as the approximated Fermi surface compared to the original are plotted in figure 2. The difference is small, and a circle makes it easy to express $\vec{k}'$ in terms of the polar angle relative to $\vec{k}$. Furthermore, due to the symmetry of the circle, $\vec{k}$ can be stationary while only $\vec{k}'$ varies. To calculate the interaction strength, let $\vec{k}$ be fixed at the point $(\frac{\pi}{2}, 0)$ and let $\vec{k}'$ run around the full Fermi surface. As a function of θ, $\vec{k}'$ is

$$\vec{k}' = \begin{bmatrix} \frac{\pi}{2}\cos(\theta) \\ \frac{\pi}{2}\sin(\theta) \end{bmatrix} \tag{120}$$

The interaction strength is then calculated as a function of θ.

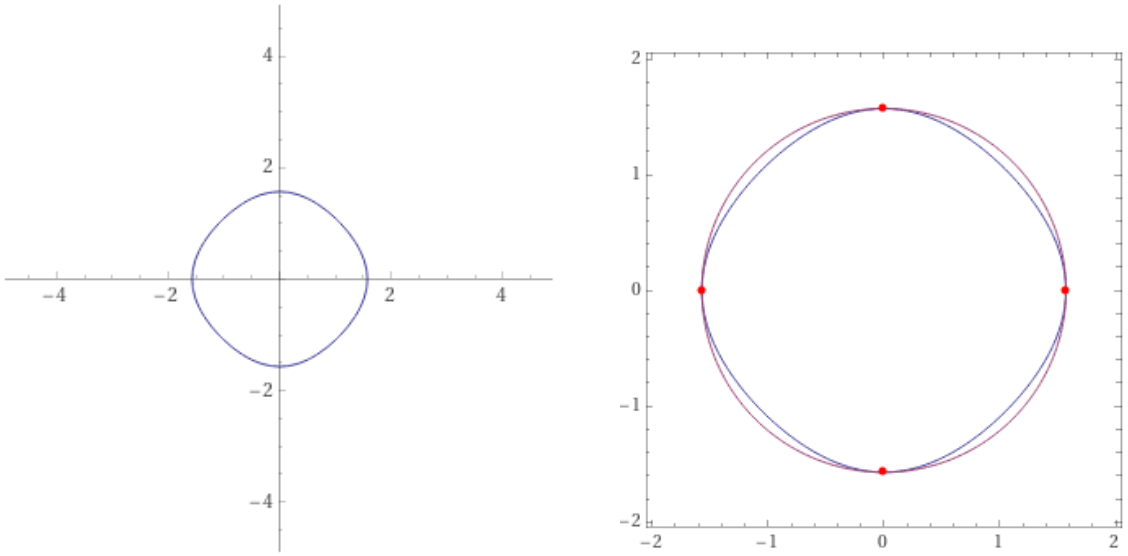

Figure 2: Left: Plot of the Fermi surface given by equation 118. Right: Plot of the approximated Fermi surface (purple) as calculated by equation 119 overlayed the real Fermi surface (blue).

5.2 Monolayer interactions

Consider first the monolayer model. The model parameters chosen for the calculations can be seen in table 1. The parameter δ refers in this case to the amount of squeezing, such that $J_y = \delta \cdot J_x$. With the parameter V is included a scaling factor such that the values of the interactions plotted are of magnitude 1. V appears only as a coefficient V^2 in every interaction, so the scaling factor does not affect the shape of the plots or the relative values of the interactions. In this section, the

Parameter	Value
J	0.25
J_x	0.05
δ	0.5
J_{sd}	0.02
t	1
V	1.5

Table 1: Model parameters for the evaluation of the interactions.

spin-triplet interaction is compared to the spin-singlet interaction, and the effect of varying the squeezing factor δ is studied.

5.2.1 Spin singlet compared to spin triplet

Firstly, it is useful to see if the spin-triplet interactions have a noticeable effect on the overall superconductivity of the material. Since the interactions are evaluated along the Fermi surface, the two spin-triplet interactions are equal in strength, as shown in section 4.1.4. Therefore only $V^{up}_{kk'}$ will be evaluated. All results are the same for $V^{down}_{kk'}$. Using the parameters in table 1, and $\vec{k}$ and $\vec{k}'$ as described above, $V^{opposite}_{kk'}$ and $V^{up}_{kk'}$ are plotted together, and their relative value calculated in figure 3.

On average along the Fermi surface, $V^{up}_{kk'}$ is only 1.02% the strength of $V^{opposite}_{kk'}$, meaning the spin-triplet interaction is on average a factor 100 weaker than the spin-singlet interaction. It is therefore reasonable to conclude that the spin-triplet interaction does not contribute in a noticeable way to the overall superconductivity of the FMI-NM material.

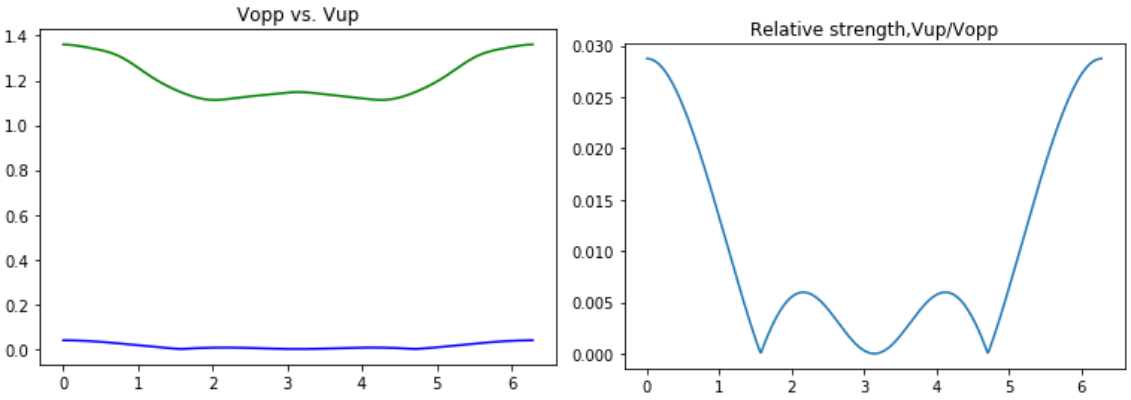

Figure 3: Left: $V_{kk'}^{opposite}$ (green) plotted together with $V_{kk'}^{up}$ (blue) on the approximated Fermi surface. Right: Plot of $V_{kk'}^{up}/V_{kk'}^{opposite}$.

5.2.2 Effect of squeezing

Consider next the effect of the amount of squeezing in the system on the interactions. Both $V_{kk'}^{opposite}$ and $V_{kk'}^{up}$ are evaluated with squeezing factors varying from $\frac{1}{4}$ to 4.

Figure 4 shows $V_{kk'}^{opposite}$ on the left and $V_{kk'}^{up}$ on the right plotted with squeezing factors 1 in blue, $\frac{1}{2}$ in yellow, $\frac{1}{3}$ in green, and $\frac{1}{4}$ in red. Figure 5 shows $V_{kk'}^{opposite}$ on the left and $V_{kk'}^{up}$ on the right plotted with squeezing factors 1 in blue, 2 in yellow, 3 in green, and 4 in red.

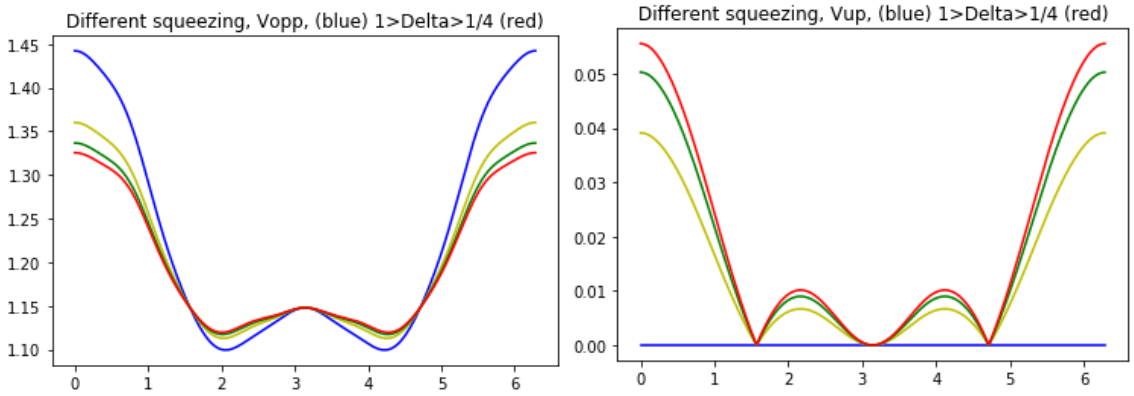

Figure 4: Left: $V_{kk'}^{opposite}$ and Right: $V_{kk'}^{up}$ plotted along the Fermi surface with squeezing factors 1 (blue), $\frac{1}{2}$ (yellow), $\frac{1}{3}$ (green) and $\frac{1}{4}$ (red).

Figures 4 and 5 shows that the spin-triplet interaction always increases when the squeezing factor moves further away from 1, which implies that it is directly related to the amount of squeezing. At no squeezing, the interaction disappears. When increasing the squeezing factor above 1, the strength increase of the interaction is also much larger than when the squeezing factor is decreased below 1. Both plots also exhibit an absolute value-like behaviour, where the interaction is zero at polar angles $\frac{\pi}{2}$, π and $\frac{3\pi}{2}$. These results are discussed further in section 6.3.

Meanwhile, $V_{kk'}^{opposite}$ has a more complex behaviour. When decreasing the squeezing factor below 1, the interaction strength decreases in the regions 0 to $\frac{\pi}{2}$ and $\frac{3\pi}{2}$ to 2π, while it increases in strength in the region $\frac{\pi}{2}$ to $\frac{3\pi}{2}$, with a local maximum at π. However, when increasing the squeezing factor above 1, the behaviours change, such that the interaction increases in strength in the regions 0 to $\frac{\pi}{2}$ and $\frac{3\pi}{2}$ to 2π, and decrease in strength in the region $\frac{\pi}{2}$ to $\frac{3\pi}{2}$. This will also be discussed further in section 6.3.

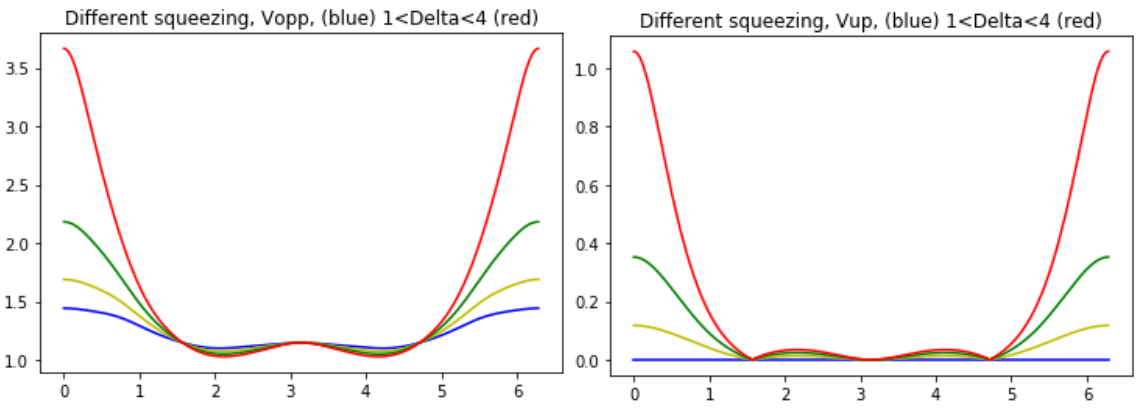

Figure 5: Left: $V_{kk'}^{opposite}$ and Right: $V_{kk'}^{up}$ plotted along the Fermi surface with squeezing factors 1 (blue), 2 (yellow), 3 (green) and 4 (red).

5.3 Two-layer interactions

In the two-layer model, the parameter J_p is introduced. This is set to $J_p = 0.04$, while all other parameters are the same as in the monolayer model, and given by table 1. In this section, the two-layer interactions are compared to the monolayer interactions, the effect of J_p is studied, and the effect of squeezing is revisited for this model.

5.3.1 Effect of multiple layers

To study the effect of including more layers of the FMI to the material, the interactions are plotted and compared to their monolayer counterparts. Figure 6 shows $V_{kk'}^{opposite}$ on the left, and $V_{kk'}^{up}$ on the right plotted in the monolayer model in blue, and the two-layer model in red.

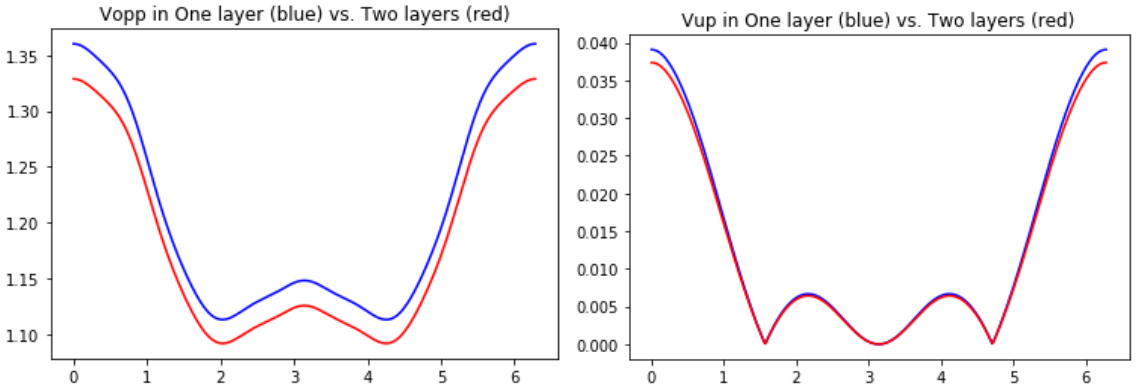

Figure 6: Left: $V_{kk'}^{opposite}$ and Right: $V_{kk'}^{up}$ plotted along the Fermi surface in the monolayer model (blue) and the two-layer model (red).

From the figure, it can be seen that both the spin-singlet and spin-triplet interactions are weaker in the two-layer model than the monolayer model. On average along the Fermi surface, $V_{kk'}^{opposite}$ in the two-layer model is 97.9% the strength of the monolayer model, while, $V_{kk'}^{up}$ in the two-layer model is 96.0% the strength of the monolayer model. Furthermore, the shape of the interactions are unchanged in the two-layer model.

5.3.2 Effect of J_p

With the introduction of the parameter J_p, its effect on the interaction strength is not immediately obvious. So the interactions are evaluated at different values of J_p to better understand it. Figure 7 shows $V_{kk'}^{opposite}$ on the left and $V_{kk'}^{up}$ on the right plotted with J_p-values 0.1 in blue, 0.075 in green, 0.05 in yellow, and 0.025 in red.

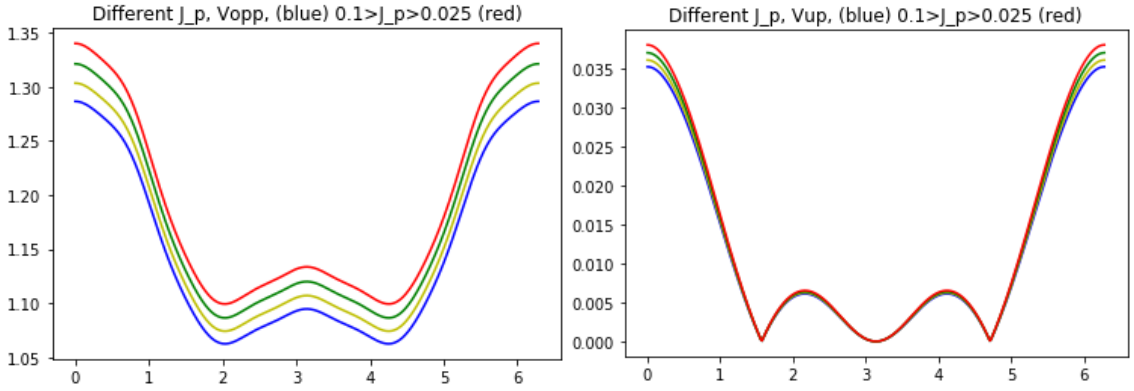

Figure 7: Left: $V_{kk'}^{opposite}$ and Right: $V_{kk'}^{up}$ plotted along the Fermi surface with J_p-values 0.1 (blue), 0.075 (yellow), 0.050 (green) and 0.025 (red).

The plots show that both the spin-singlet and spin-triplet interactions decrease in strength with an increasing value of J_p. Going from $J_p = 0.025$ to $J_p = 0.1$, $V_{kk'}^{opposite}$ decreases to an average of 96.4% of its strength, while $V_{kk'}^{up}$ decreases to an average of 93.3% of its strength. The shape of the plots are unchanged

5.3.3 Effect of squeezing

Consider next the effect of squeezing on the two-layer FMI. The sqeezing factor varies between $\frac{1}{4}$ and 4. Figure 8 shows $V_{kk'}^{opposite}$ to the left and $V_{kk'}^{up}$ to the right plotted with squeezing factors 1 in blue, $\frac{1}{2}$ in yellow, $\frac{1}{3}$ in green, and $\frac{1}{4}$ in red. Figure 9 shows $V_{kk'}^{opposite}$ on the left, and $V_{kk'}^{up}$ on the right plotted with squeezing factors 1 in blue, 2 in yellow, 3 in green, and 4 in red.

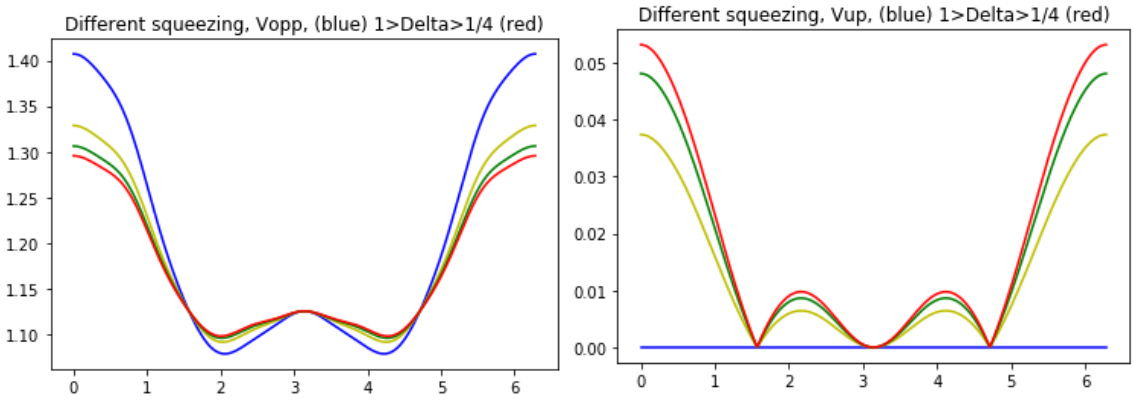

Figure 8: Left: $V_{kk'}^{opposite}$ and Right: $V_{kk'}^{up}$ plotted along the Fermi surface with squeezing factors 1 (blue), $\frac{1}{2}$ (yellow), $\frac{1}{3}$ (green) and $\frac{1}{4}$ (red).

Comparing these figures with figures 4 and 5, the behaviour of the interactions at different squeezing factors, as well as the shape of the curves are almost identical. This implies that the effect of squeezing on the interactions does not change in a noticeable way when including a second layer to the FMI.

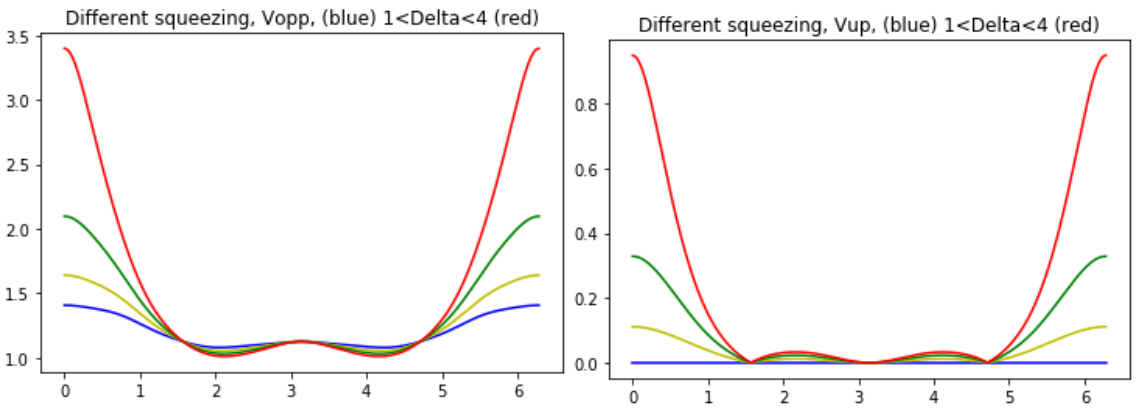

Figure 9: Left: $V_{kk'}^{opposite}$ and Right: $V_{kk'}^{up}$ plotted along the Fermi surface with squeezing factors 1 (blue), 2 (yellow), 3 (green) and 4 (red).

In summary, this section has shown that the spin-triplet interaction is about 1% the strength of the spin-singlet interaction, that the spin-triplet interaction increases in strength the further away from 1 the squeezing factor is, that the spin-singlet interaction increases in strength with an increasing squeezing factor in one region and decreases in strength in another region of the Fermi surface, and that both the presence and increase of J_p reduces both interaction strengths.

6 Discussion

This section will attempt to explain why the interactions behave as they do when changing the system parameters, as well as explain where the spin-triplet interactions come from.

6.1 Origin of the spin-triplet interaction

As reported in sections 4.1.3 and 4.2.3, the models exhibit two additional spin-triplet interactions that are not predicted by the BCS-model.

To see where these come from, consider the original form of $H_1^{(k)}$ in the FMI model after the spin-flip operators have been introduced. This is given by

$$H_1^{(k)} = -\sum_{<i,j>} [JS_{iz}^k S_{jz}^k + \frac{1}{2}\overline{J}(S_{i+}^k S_{j-}^k + S_{i-}^k S_{j+}^k) + \frac{1}{2}\Delta J(S_{i+}^k S_{j+}^k + S_{i-}^k S_{j-}^k)], \tag{121}$$

where $2\overline{J} = J_x + J_y$ and $2\Delta J = J_x - J_y$. The final term is proportional to ΔJ and contains the spin-flip operator structure $S_{i+}^k S_{j+}^k + S_{i-}^k S_{j-}^k$, which flips two neighbouring FMI spins up and two down. The magnons associated with this process are kept when Bogoliubov transforming the Hamiltonian, such that the operators representing long-lived operators, A_q and $A_q^\dagger$, also contain terms that represent spin flipping two neighbouring spins either up or down. When these are connected to the electrons of the NM via the coupling Hamiltonian

$$H_c = -J_{sd}\sum_i \vec{S}_i^1 \cdot \vec{s}_i, \tag{122}$$

the electrons at lattice sites i and j also flip. This is because since J_{sd} is positive, the energy is minimized when the spins are parallel. A double spin flip in the top layer of the FMI then leads to a double spin flip in the electrons as well. A double spin flip in the second layer connects to the first layer via the interlayer coupling term

$$H_2^{1,2} = -J_p\sum_i \vec{S}_i^1 \cdot \vec{S}_i^2, \tag{123}$$

and then to the electrons in the normal metal via equation 122. The magnons from the double spin flip thus leads to spin triplet Cooper pairs.

6.2 Effect of J_p and multiple layers

In figure 6 it can be seen that both $V_{kk'}^{opposite}$ and $V_{kk'}^{up}$ (as well as $V_{kk'}^{down}$) are weaker in the two-layer model than the monolayer model. Furthermore, figure 7 shows that the interactions decrease in strength with an increasing value of J_p. This section aims to provide both a mathematical and a physical explanation for the behaviour. For the following discussion, let u_q, v_q and ω_q refer to the monolayer values, and let u_{qi}, v_{qi} and ω_{qi}, where $i = 1, 2$, refer to the values in the two-layer FMI. For simplicity of notation, write q instead of $k - k'$ as index.

6.2.1 Spin-singlet interaction

Consider first the spin-singlet interaction. Since the interaction is evaluated at the Fermi surface, such that $(\varepsilon_k - \varepsilon_{k'}) = 0$, equation 113 reduces to

$$V_{kk',2}^{opposite} = \sum_{i=1}^{2} \big[\frac{V^2 u_{qi}^2}{\tilde{\omega}_{qi}^-} + \frac{V^2 v_{qi}^2}{\tilde{\omega}_{qi}^+}\big], \tag{124}$$

where the subscript 2 refers to this being in the two-layer model. In this expression, the only dependence on J_p appears in the $i = 2$ term, through $\Delta = \frac{1}{2} J_p S$. To mathematically understand the behaviour, the explicit dependence on Δ will be considered. The expressions for u_{q2} and v_{q2} are

$$u_{q2} = \sqrt{\frac{2(C_q + 2\Delta) + \omega_{q2}}{4\omega_{q2}}}, \tag{125}$$

$$v_{q2} = \sqrt{\frac{2(C_q + 2\Delta) - \omega_{q2}}{4\omega_{q2}}}, \tag{126}$$

where

$$\omega_{q2} = 2\sqrt{(C_q + 2\Delta)^2 - D_q^2}. \tag{127}$$

All the dependence on Δ appears as $(C_q + 2\Delta)$. Let there instead be a variable dependence on Δ, by setting $2\Delta \to x\Delta$, where x is a non-negative real number. The expressions then read

$$u_{q2}(x) = \sqrt{\frac{2(C_q + x\Delta) + \omega_{q2}}{4\omega_{q2}}}, \tag{128}$$

$$v_{q2}(x) = \sqrt{\frac{2(C_q + x\Delta) - \omega_{q2}}{4\omega_{q2}}}, \tag{129}$$

where

$$\omega_{q2}(x) = 2\sqrt{(C_q + x\Delta)^2 - D_q^2}. \tag{130}$$

Notice that $u_{q2}(0) = u_{q1}$, $v_{q2}(0) = v_{q1}$ and $\omega_{q2}(0) = \omega_{q1}$. Furthermore, by the positivity of the square root, all these functions are non-negative. This also extends to $\tilde{\omega}_{qi}^{\pm} = \omega_{qi} \pm 2(h + J_{sd}S)$ for reasonable values of h and J_{sd} as well. Moreover, the functions $C_q = JSz - \overline{J}S\gamma(\vec{q})$ and Δ are also positive within the system specifications. Differentiating the functions with respect to x, one gets

$$\frac{\partial \omega_{q2}}{\partial x} = \frac{4\Delta(C_q + x\Delta)}{\omega_{q2}} > 0, \tag{131}$$

$$\frac{\partial u_{q2}}{\partial x} = -\frac{\Delta D_q^2}{4u_{q2}\omega_{q2}^3} < 0, \tag{132}$$

$$\frac{\partial v_{q2}}{\partial x} = \frac{u_{q2}}{v_{q2}}\frac{\partial u_{q2}}{\partial x} = -\frac{\Delta D_q^2}{4v_{q2}\omega_{q2}^3} < 0. \tag{133}$$

Thus, differentiating $V_{kk',2}^{opposite}$ yields

$$\frac{\partial V_{kk',2}^{opposite}}{\partial x} = V^2\Big[\frac{2u_{q2}\tilde{\omega}_{q2}^- \frac{\partial u_{q2}}{\partial x} - u_{q2}^2\frac{\partial \tilde{\omega}_{q2}^-}{\partial x}}{(\tilde{\omega}_{q2}^-)^2} + \frac{2v_{q2}\tilde{\omega}_{q2}^+ \frac{\partial v_{q2}}{\partial x} - v_{q2}^2\frac{\partial \tilde{\omega}_{q2}^+}{\partial x}}{(\tilde{\omega}_{q2}^+)^2}\Big] < 0. \tag{134}$$

Every term in the numerators are negative, meaning the overall expression is negative. This shows mathematically that $V_{kk',2}^{opposite}$ decreases with an increasing dependence on J_p.

Relate this to $V_{kk',1}^{opposite}$ by noting that since $x = 0$ gives the $i = 1$ values of the corresponding functions, the $i = 1$ term of $V_{kk',2}^{opposite}$ is larger than the $i = 2$ term. In addition, as stated in section 4.2.1, one has the relationships

$$\begin{aligned} u_{q1} &= \frac{1}{\sqrt{2}}u_q, \\ v_{q1} &= \frac{1}{\sqrt{2}}v_q, \\ \omega_{q1} &= \omega_q, \end{aligned} \tag{135}$$

meaning the $i = 1$ term of $V_{kk',2}^{opposite}$ is exactly half the value of $V_{kk',1}^{opposite}$. Since the $i = 2$ term is smaller, one gets that $V_{kk',2}^{opposite}$ must be weaker than $V_{kk',1}^{opposite}$. This is a direct consequence of introducing J_p to the system.

Physically, this can be explained by how the FMI connects to the NM. The model for the FMI-NM coupling is

$$H = -V\sum_{k,q}\big[a_q c_{k+q,\downarrow}^\dagger c_{k\uparrow} + a_{-qk+q,\uparrow}^\dagger c_{k\downarrow}\big]. \tag{136}$$

Since the magnons of layer 2 represented by b_q are not directly coupled to the NM, they do not directly mediate Cooper pairs. Instead, the magnons of layer 2 interact with the magnons of layer 1 through J_p to mediate Cooper pairs. Due to the extra step, this should be a weaker electron-magnon interaction than the direct coupling of the magnons of layer 1 to the NM. This means that a normalized linear combination of a_q and b_q will be weaker than a_q alone. Thus, the normalized linear combinations, A_q and B_q, of the a_q- and b_q operators will in general result in weaker interactions than the magnons represented by a_q alone does. Since J_p is the exchange interaction coupling the a_q-magnons to the b_q-magnons, the stronger it is, the more b_q contributes to A_q and B_q. The result is that the A_q- and B_q-magnons give rise to a weaker electron-magnon coupling due to a larger presence of the b_q-magnons when J_p increases. However, the author is unaware of studies discussing this specific effect, meaning there is no scientific evidence to further prove/disprove this theory.

6.2.2 Spin-triplet interaction

Consider next the spin-triplet interactions. On the Fermi surface, since $(\varepsilon_k - \varepsilon_{k'}) = 0$, the spin-triplet interactions in the two-layer model can be written as

$$V_{kk',2}^{up} = V_{kk',2}^{down} = V^2\sum_{i=1}^{2}\frac{u_{qi}v_{qi}\omega_{qi}}{\tilde{\omega}_{qi}^+\tilde{\omega}_{qi}^-}, \tag{137}$$

where $\tilde{\omega}_{qi}^\pm = \omega_{qi} \pm 2m$, $m = h + SJ_{sd}$, and the subscript 2 indicates that this is in the two-layer model.

Let again $2\Delta \to x\Delta$ and use the expressions for $u_{q2}(x)$, $v_{q2}(x)$ and $\omega_{q2}(x)$ as given by equations 128, 129 and 130. Differentiating $V_{kk',2}^{up}$ with respect to x yields

$$\frac{\partial V_{kk',2}^{up}}{\partial x} = -\frac{\Delta|D_q|(C_q + x\Delta)}{2\omega_{q2}^2(\tilde{\omega}_{q2}^+\tilde{\omega}_{q2}^-)^2}\big(\omega_{q2}^2 + 6m^2\big) < 0, \tag{138}$$

which shows that also the spin-triplet interaction decreases with dependence on J_p. This means that the $i = 1$ term is larger than the $i = 2$ term. The $i = 1$ term is also exactly half the strength of $V^{up}_{kk',1}$, and since the $i = 2$ term is smaller, this means that $V^{up}_{kk',2}$ as a whole is weaker than $V^{up}_{kk',1}$.

Physically, the explanation is the same as the one provided for the spin-singlet interaction in section 6.2.1.

6.3 Effect of squeezing

Consider finally how the squeezing affects the interactions. Since the effect of the squeezing did not change when going from one to two layers, the main focus of this section is the monolayer interactions. The arguments are identical for the two-layer interactions.

6.3.1 Spin-singlet interaction

Consider first the spin-singlet interaction. From equation 121, it can be seen that the spin-flip operators that give rise to the spin-singlet interaction is proportional to $\overline{J} = \frac{J_x+J_y}{2}$. Naïvely, this should mean that the strength of the spin-singlet interaction increases when the sum $J_x + J_y$ increases. Thus, since a squeezing factor smaller than 1 decreases J_y, the interaction should be weaker. Similarly, since a squeezing factor larger than 1 increases J_y, the interaction should be stronger. However, this only applies to the regions where θ lies on the intervals 0 to $\frac{\pi}{2}$ and $\frac{3\pi}{2}$ to 2π. On the interval $\frac{\pi}{2}$ to $\frac{3\pi}{2}$, the opposite is true. To explain this, consider the expression for $V^{opposite}_{kk'}$ on the Fermi surface, given by

$$V^{opposite}_{kk'} = V^2\Big(\frac{u_q^2}{\tilde{\omega}_q^-} + \frac{v_q^2}{\tilde{\omega}_q^+}\Big). \tag{139}$$

Rewrite it in terms of the values C_q, D_q and m, giving

$$V^{opposite}_{kk'} = \frac{V^2}{2}\frac{C_q + m}{(C_q^2 - m^2) - D_q^2}, \tag{140}$$

where $C_q = JSz - \overline{J}S\gamma(\vec{q})$, $D_q = -\Delta JS\gamma(\vec{q})$ and $m = h + J_{sd}S$. Differentiating this expression with respect to J_y gives

$$\frac{\partial V^{opposite}_{kk'}}{\partial J_y} = S\gamma(\vec{q})\frac{J_y}{2}\cdot \underbrace{\frac{(C_q + m)(C_q + D_q) - \tilde{\omega}_q^+\tilde{\omega}_q^-}{(\tilde{\omega}_q^+\tilde{\omega}_q^-)^2}}_{\lambda_q}. \tag{141}$$

Setting $\vec{q} = \vec{k} - \vec{k}'$, where $\vec{k} = \big[\frac{\pi}{2}, \quad 0\big]$ and $\vec{k}' = \big[\frac{\pi}{2}\cos\theta, \quad \frac{\pi}{2}\sin\theta\big]$, the sign of λ_q does not change as a function of θ. However, the sign of $\gamma(\vec{q})$ is positive on the intervals 0 to $\frac{\pi}{2}$ and $\frac{3\pi}{2}$ to 2π, and negative on the interval $\frac{\pi}{2}$ to $\frac{3\pi}{2}$. Thus, the interaction behaves oppositely with respect to the size of J_y in these regions. While this can be seen as an effect of squeezing, it is not directly dependent on the difference $J_x - J_y$. Instead, it depends on the value of J_y alone. Combining this with the fact that the spin-flip operators are proportional to $J_x + J_y$, it seems to be more related to the value of $J_x + J_y$ instead of the absolute value of $J_x - J_y$.

Considering $\gamma(\vec{q})$ further, it is zero at the θ-values $\frac{\pi}{2}$, π and $\frac{3\pi}{2}$, which explains why the interaction does not vary with squeezing factor at these points.

6.3.2 Spin-triplet interaction

Consider next the spin-triplet interactions. Firstly, as discussed in section 6.1, the spin-flip operators that give rise to the spin-triplet interactions are proportional to $\Delta J = \frac{J_x-J_y}{2}$. When $J_x = J_y$,

$\Delta J = 0$, which explains why the interactions are 0 for squeezing factor 1. However, looking at the expression for the interactions gives more information. On the Fermi surface, the expressions reduce to

$$V_{kk'}^{up} = V_{kk'}^{down} = V^2 \frac{u_q v_q \omega_q}{\tilde{\omega}_q^+ \tilde{\omega}_q^-}. \tag{142}$$

Rewriting the expression in terms of C_q, D_q and m gives

$$V_{kk'}^{up} = V_{kk'}^{down} = V^2 \frac{|D_q|}{4(C_q^2 - m^2) - 4D_q^2}, \tag{143}$$

where $C_q = JSz - \overline{J}S\gamma(\vec{q})$, $D_q = -\Delta JS\gamma(\vec{q})$ and $m = h + J_{sd}S$.

Since D_q is a real value, $D_q^2 = |D_q|^2$, which means the spin-triplet interactions are purely dependent on $|D_q| = S|\Delta J||\gamma(\vec{q})|$. In particular, the spin-triplet interactions are only dependent on $|\Delta J|$, and not ΔJ. Both the numerator and the inverse of the denominator of equation 143 increase with an increasing $|D_q|$, which means that $V_{kk'}^{up}$ and $V_{kk'}^{down}$ increase with an increasing value of $|\Delta J|$. Thus, both reducing the squeezing factor below 1 and increasing the squeezing factor above 1 yields a stronger interaction as $|\Delta J|$ becomes larger either way. As for why the interaction increases more when the squeezing factor is larger than 1 than when the squeezing factor is smaller than 1, consider ΔJ expressed in terms of the squeezing factor δ. The relation is

$$\Delta J = \frac{J_x}{2}(1 - \delta). \tag{144}$$

For $\delta = 4$, the value is $|\Delta J(\delta = 4)| = \frac{3J_x}{2}$, while $\delta = \frac{1}{4}$ gives $|\Delta J(\delta = \frac{1}{4}) = \frac{3J_x}{8} = \frac{1}{4} \cdot |\Delta J(\delta = 4)|$. Since the gap between J_x and J_y in absolute value is larger for squeezing factor 4 than $\frac{1}{4}$, $|D_q|$, and in turn $V_{kk'}^{up}$ also become larger.

This approach also explains the shape of the spin-triplet interactions. The shape comes from the $|\gamma(\vec{q})|$ in the numerator. Setting $\vec{q} = \vec{k} - \vec{k}'$, where $\vec{k} = \left[\frac{\pi}{2}, \quad 0\right]$ and $\vec{k}' = \left[\frac{\pi}{2}\cos\theta, \quad \frac{\pi}{2}\sin\theta\right]$, the zeros of $|\gamma(\vec{q})|$ are when θ is $\frac{\pi}{2}$, π and $\frac{3\pi}{2}$, which are the same as seen in section 5.

7 Conclusion

The paper studied the magnon-mediated effective electron-electron interaction in a FMI-NM heterostructure using the BCS model. In particular, the effects of adding a second layer to the FMI, and the effect of an anisotropic exchange interaction (squeezing) in the FMI on the electron-magnon interaction were studied. In addition to spin-singlet Cooper pairs, spin-triplet Cooper pairs were discovered in the model and found to form as a direct consequence of the squeezing. When adding a second layer of the FMI to the model, all interactions were found to decrease in strength. This was related to the strength of the interlayer coupling J_p, where a larger J_p lead to weaker interactions. Reasons for this were discussed and shown to result in weaker interactions in the two-layer FMI model than the monolayer model. When varying the amount of squeezing, the spin-triplet interactions were found to increase in strength with an increasing amount of squeezing. Meanwhile, the spin-singlet interaction was found to depend on the sum of J_x and J_y instead of their difference. On one region of the Fermi surface, it increases with an increasing sum, while on the complementary region it decreases with an increasing sum. This was shown mathematically. The effect of squeezing was the same for one layer as for two layers of the FMI.

In conclusion, the strongest e-e interaction is achieved by having a monolayer FMI where both the anisotropic exchange interactions, J_x and J_y, are maximized. Since the spin-triplet interaction is 1% the strength of the spin-singlet interaction, the contributions to the overall superconductivity is negligable. Thus, the superconducting properties of the FMI-NM heterostructure are maximized when the spin-singlet interaction is prioritized. Hopefully, this can provide further insight into superconductivity and some day even contribute to room-temperature superconductors.

Bibliography

[1] R. Combescot, *Superconductivity*. Cambridge university press, 2022.

[2] J. Wirfs-Brock, "Lost in transmission: How much electricity disappears between a power plant and your plug?" *Inside Energy*, 2015. [Online]. Available: http://insideenergy.org/2015/11/06/lost-in-transmission-how-much-electricity-disappears-between-a-power-plant-and-your-plug/.

[3] W. Meissner and R. Ochsenfeld, "Ein neuer effekt bei eintritt der supraleitfähigkeit," *Naturwissenschaften*, 1933. DOI: https://doi.org/10.1007/BF01504252.

[4] C. Whyte, "How maglev works," 2016. [Online]. Available: https://www.energy.gov/articles/how-maglev-works.

[5] I. Dixon, "Superconducting magnet," 2014. [Online]. Available: https://nationalmaglab.org/about/maglab-dictionary/superconducting-magnet.

[6] J. P. Hornak, "The basics of nmr, chapter 7: Nmr hardware," 2017. [Online]. Available: https://www.cis.rit.edu/htbooks/nmr/chap-7/chap-7.htm.

[7] A. Murphy, "Magnets (types)," 2020. [Online]. Available: https://radiopaedia.org/articles/magnets-types.

[8] CERN, "Pulling together: Superconducting electromagnets," [Online]. Available: https://home.cern/science/engineering/pulling-together-superconducting-electromagnets.

[9] B. T. Matthias, T. H. Geballe, and V. B. Compton, "Superconductivity," *Reviews of modern physics*, vol. 35, 1963. DOI: https://doi.org/10.1103/RevModPhys.35.1.

[10] D. van Delft and P. Kes, "The discovery of superconductivity," *physics today*, vol. 63, 2010. DOI: https://doi.org/10.1063/1.3490499.

[11] J. von Neumann, *Mathematical Foundations of Quantum Mechanics*. Princeton University Press, 1932.

[12] E. Maxwell, "Isotope effect in the superconductivity of mercury," *Phys. Rev.*, vol. 78, 1950. DOI: https://doi.org/10.1103/PhysRev.78.477.

[13] J. Bardeen, L. N. Cooper, and J. R. Schrieffer, "Theory of superconductivity," *Phys. Rev.*, vol. 108, 1957. DOI: https://doi.org/10.1103/PhysRev.108.1175.

[14] A. Sudbø, A. Brataas, and E. Erlandsen, "Magnon-mediated superconductivity on the surface of a topological insulator," *Phys. Rev. B*, vol. 101, 2020. DOI: https://doi.org/10.1103/PhysRevB.101.094503.

[15] R. Kar, B. C. Paul, and A. Misra, "Unconventional superconductivity in iron pnictides: Magnon mediated pairing," *Physica C*, vol. 545, 2018. DOI: https://doi.org/10.1016/j.physc.2017.11.008.

[16] N. Karchev, "Magnon-mediated superconductivity in itinerant ferromagnets," *J. Phys.: Condens. Matter*, vol. 15, 2003.

[17] A. Kavokin and P. Lagoudakis, "Exciton-mediated superconductivity," *Nature Mater*, vol. 15, 2016. DOI: https://doi.org/10.1038/nmat4646.

[18] P. Fabrice, A. V. Kavokin, and I. A. Shelykh, "Exciton-polariton mediated superconductivity," *Phys. Rev. Lett.*, vol. 104, 2009. DOI: https://doi.org/10.1103/PhysRevLett.104.106402.

[19] A. Davydov, A. Sanna, C. Pellegrini, J. K. Dewhurst, S. Sharma, and E. K. U. Gross, "Ab initio theory of plasmonic superconductivity within the eliashberg and density-functional formalisms," *Phys. Rev. B*, vol. 102, 2020. DOI: https://doi.org/10.1103/PhysRevB.102.214508.

[20] A. Mukubwa and J. W. Makokha, "Plasmon mediation of charge pairing in high temperature superconductors," *Advances in Condensed Matter Physics*, vol. 2021, 2021. DOI: https://doi.org/10.1155/2021/7234840.

[21] J. G. Bednorz and K. A. Müller, "Possible highT_c superconductivity in the balacuo system," *Zeitschrift für Physik B Condensed Matter*, vol. 64, 1986. DOI: https://doi.org/10.1007/BF01303701.

[22] Y. Kamihara, H. Hiramatsu, M. Hirano, *et al.*, "Iron-based layered superconductor: laofep," *J. Am. Chem. Soc.*, vol. 128, 2006. DOI: https://doi.org/10.1021/ja063355c.

[23] P. W. Anderson, G. Baskaran, Z. Zou, and T. Hsu, "Resonating–valence-bond theory of phase transitions and superconductivity in La_2CuO_4-based compounds," *Phys. Rev. Lett.*, vol. 58, 1987. DOI: https://doi.org/10.1103/PhysRevLett.58.2790.

[24] K. M. Shen and J. S. Davis, "Cuprate high-tc superconductors," *Materials Today*, vol. 11, no. 9, pp. 14–21, 2008, ISSN: 1369-7021. DOI: https://doi.org/10.1016/S1369-7021(08)70175-5. [Online]. Available: https://www.sciencedirect.com/science/article/pii/S1369702108701755.

[25] R. Yan, G. Khalsa, S. Vishwanath, *et al.*, "Gan/nbn epitaxial semiconductor/superconductor heterostructures," *Nature*, vol. 555, pp. 183–189, 2018. DOI: https://doi.org/10.1038/nature25768.

[26] Y.-M. Xie, K. T. Law, and P. A. Lee, "Topological superconductivity in eus/au/superconductor heterostructures," *Phys. Rev. Research*, vol. 3, 4 2021. DOI: 10.1103/PhysRevResearch.3.043086. [Online]. Available: https://link.aps.org/doi/10.1103/PhysRevResearch.3.043086.

[27] S. D. Escribano, A. Maiani, M. Leijnse, *et al.*, "Semiconductor-ferromagnet-superconductor planar heterostructures for 1d topological superconductivity," 2022. DOI: https://doi.org/10.48550/arxiv.2203.06644. [Online]. Available: https://arxiv.org/abs/2203.06644.

[28] O. Lesser, A. Saydjari, M. Wesson, A. Yacoby, and Y. Oreg, "Phase-induced topological superconductivity in a planar heterostructure," *Proceedings of the National Academy of Sciences*, vol. 118, no. 27, 2021. DOI: 10.1073/pnas.2107377118.

[29] I. Garifullin, "Proximity effects in ferromagnet/superconductor heterostructures," *Journal of Magnetism and Magnetic Materials*, vol. 240, no. 1, pp. 571–576, 2002, ISSN: 0304-8853. DOI: https://doi.org/10.1016/S0304-8853(01)00849-6. [Online]. Available: https://www.sciencedirect.com/science/article/pii/S0304885301008496.

[30] R. Ramesh, A. Inam, W. K. Chan, *et al.*, "Epitaxial cuprate superconductor/ferroelectric heterostructures," *Science*, vol. 252, no. 5008, pp. 944–946, 1991. DOI: 10.1126/science.252.5008.944.

[31] R. M. Lutchyn, J. D. Sau, and S. D. Sarma, "Majorana fermions and a topological phase transition in semiconductor-superconductor heterostructures," *Physical Review Letters*, vol. 105, no. 7, 2010. DOI: 10.1103/physrevlett.105.077001.

[32] K. Roy, A. Mishra, P. Gupta, S. Mohanty, B. Singh, and S. Bedanta, "Spin pumping and inverse spin hall effect in cofeb/irmn heterostructures," *Journal of Physics D Applied Physics*, vol. 54, 2021. DOI: 10.1088/1361-6463/ac153a.

[33] D. Jhajhria, N. Behera, D. K. Pandya, and S. Chaudhary, "Dependence of spin pumping in w/cofeb heterostructures on the structural phase of tungsten," *Phys. Rev. B*, vol. 99, 1 2019. DOI: 10.1103/PhysRevB.99.014430.

[34] A. Dankert and S. Dash, "Electrical gate control of spin current in van der waals heterostructures at room temperature," *Nat Commu*, vol. 8, 2017. DOI: https://doi.org/10.1038/ncomms16093.

[35] C. N. Wu, Y. H. Lin, Y. T. Fanchiang, *et al.*, "Strongly enhanced spin current in topological insulator/ferromagnetic metal heterostructures by spin pumping," *Journal of Applied Physics*, vol. 117, 2015. DOI: https://doi.org/10.1063/1.4918631.

[36] B. Huang, M. A. McGuire, A. F. May, D. Xiao, P. Jarillo-Herrero, and X. Xu, "Emergent phenomena and proximity effects in two-dimensional magnets and heterostructures," *Nature Materials*, vol. 19, 2020. DOI: https://doi.org/10.1038/s41563-020-0791-8.

[37] H. Han, J. Ling, W. Liu, H. Li, C. Zhang, and J. Wang, "Superconducting proximity effect in a van der waals 2h-tas2/nbse2 heterostructure," *Appl. Phys. Lett.*, vol. 118, 2021. DOI: https://doi.org/10.1063/5.0051968.

[38] N. Rohling, E. L. Fjærbu, and A. Brataas, "Superconductivity induced by interfacial coupling to magnons," *Phys. Rev. B*, vol. 97, 11 2018. DOI: 10.1103/PhysRevB.97.115401. [Online]. Available: https://link.aps.org/doi/10.1103/PhysRevB.97.115401.

[39] E. L. Fjærbu, N. Rohling, and A. Brataas, "Superconductivity at metal-antiferromagnetic insulator interfaces," *Physical Review B*, vol. 100, no. 12, 2019. DOI: 10.1103/physrevb.100.125432.

[40] M. Kargarian, D. K. Efimkin, and V. Galitski, "Amperean pairing at the surface of topological insulators," *Phys. Rev. Lett.*, vol. 117, 7 2016. DOI: 10.1103/PhysRevLett.117.076806.

[41] H. G. Hugdal, S. Rex, F. S. Nogueira, and A. Sudbø, "Magnon-induced superconductivity in a topological insulator coupled to ferromagnetic and antiferromagnetic insulators," *Phys. Rev. B*, vol. 97, 19 2018. DOI: 10.1103/PhysRevB.97.195438.

[42] E. Erlandsen, A. Kamra, A. Brataas, and A. Sudbø, "Enhancement of superconductivity mediated by antiferromagnetic squeezed magnons," *Physical Review B*, vol. 100, no. 10, 2019. DOI: 10.1103/physrevb.100.100503.

[43] A. Kamra and W. Belzig, "Super-poissonian shot noise of squeezed-magnon mediated spin transport," *Phys. Rev. Lett.*, vol. 116, 14 2016. DOI: 10.1103/PhysRevLett.116.146601.

[44] J. Yang, J. Luo, C. Yi, Y. Shi, Y. Zhou, and G.-q. Zheng, "Spin-triplet superconductivity in k2cr3as3," *Science Advances*, vol. 7, no. 52, 2021. DOI: 10.1126/sciadv.abl4432.

[45] S. Ran, C. Eckberg, Q.-P. Ding, *et al.*, "Nearly ferromagnetic spin-triplet superconductivity," *Science*, vol. 365, no. 6454, pp. 684–687, 2019. DOI: 10.1126/science.aav8645.

[46] V. Crépel and L. Fu, "Spin-triplet superconductivity from excitonic effect in doped insulators," *Proceedings of the National Academy of Sciences*, vol. 119, no. 13, 2022. DOI: 10.1073/pnas.2117735119.

[47] T. Shang, S. K. Ghosh, M. Smidman, *et al.*, "Spin-triplet superconductivity in weyl nodal-line semimetals," *npj Quantum Mater*, vol. 7, no. 35, 2022. DOI: https://doi.org/10.1038/s41535-022-00442-w.

[48] Y. Xu, Y. Sheng, and Y.-f. Yang, "Quasi-two-dimensional fermi surfaces and unitary spin-triplet pairing in the heavy fermion superconductor UTe_2," *Phys. Rev. Lett.*, vol. 123, 21 2019. DOI: 10.1103/PhysRevLett.123.217002.

[49] D. Bishop and I. Ismail, "Metallic superconductors," in *Reference Module in Materials Science and Materials Engineering*, Elsevier, 2016, ISBN: 978-0-12-803581-8. DOI: https://doi.org/10.1016/B978-0-12-803581-8.01272-8.

[50] C. Tsallis, "Diagonalization methods for the general bilinear hamiltonian of an assembly of bosons," *J. Math. Phys.*, vol. 19, 1978. DOI: https://doi.org/10.1063/1.523549.

[51] O. Maldonado, "On the bogoliubov transformation for quadratic boson observables," *J. Math. Phys.*, vol. 34, 1998. DOI: https://doi.org/10.1063/1.530338.

[52] J. R. Schrieffer and P. A. Wolff, "Relation between the anderson and kondo hamiltonians," *Phys. Rev.*, vol. 149, 1966.

[53] S. Bravyi, D. P. DiVincenzo, and D. Loss, "Schrieffer-wolff transformation for quantum many-body systems," *Annals of Physics*, vol. 326, no. 10, pp. 2793–2826, 2011. DOI: 10.1016/j.aop.2011.06.004.

[54] L. N. Cooper, "Bound electron pairs in a degenerate fermi gas," *Phys. Rev.*, vol. 104, pp. 1189–1190, 4 1956. DOI: 10.1103/PhysRev.104.1189.

[55] T. Holstein and H. Primakoff, "Field dependence of the intrinsic domain magnetization of a ferromagnet," *Phys. Rev.*, vol. 58, 12 1940. DOI: 10.1103/PhysRev.58.1098.

Appendix

A Deriving the SW transformation

Let S be the generator for the transformation. If H_1 is small, then so will S be too. The transformation is then

$$H' = e^{-S} H e^{S}. \tag{145}$$

Taylor-expand the exponentials and gather the terms to get

$$\begin{aligned} H' &= (1 - S + \frac{1}{2}S^2 - ...)(H_0 + H_1)(1 + S + \frac{1}{2}S^2 + ...) \\ &= H_0 + H_1 + H_0 S - S H_0 + H_1 S - S H_1 + \frac{1}{2}H_0 S^2 - S H_0 S + \frac{1}{2}S^2 H_0 + O(H_1^3) \\ &= H_0 + H_1 + [H_0, S] + [H_1, S] + \frac{1}{2}[H_0, S]S - \frac{1}{2}S[H_0, S] + O(H_1^3) \\ &= H_0 + H_1 + [H_0, S] + [H_1, S] + \frac{1}{2}[[H_0, S], S] + O(H_1^3) \end{aligned} \tag{146}$$

Choose S such that $[H_0, S] = -H_1$ and the expression collapses into

$$\begin{aligned} &= H_0 + H_1 - H_1 + [H_1, S] + \frac{1}{2}[-H_1, S] + O(H_1^3) \\ &= H_0 + \frac{1}{2}[H_1, S] + O(H_1^3) \end{aligned} \tag{147}$$

The Schieffer-Wolff transformed Hamiltonian is then

$$H' = H_0 - \frac{1}{2}[S, H_1], \tag{148}$$

where the order of the commutator is changed.

B Bogoliubov transformation of H_{FM} in monolayer model

The FMI-Hamiltonian in the monolayer model is given by

$$H_{FM} = E_0^* + \sum_q \begin{bmatrix} a_q^\dagger, & a_{-q} \end{bmatrix} \begin{bmatrix} C_q & D_q \\ D_q & C_q \end{bmatrix} \begin{bmatrix} a_q \\ a_{-q}^\dagger \end{bmatrix}, \tag{149}$$

where $E_0^* = -JNzS^2 - \sum_q C_q$. Following the method presented in section 2.2, this section derives the Bogoliubov transformed Hamiltonian. The matrix

$$PJ = \begin{bmatrix} C_q & -D_q \\ D_q & -C_q \end{bmatrix} \tag{150}$$

has eigenvalues

$$\begin{cases} \lambda_1 = \sqrt{C_q^2 - D_q^2} \\ \lambda_2 = -\sqrt{C_q^2 - D_q^2} \end{cases}, \tag{151}$$

which will be denoted by $\pm\lambda$, where $\lambda = \sqrt{C_q^2 - D_q^2}$. The corresponding eigenvectors are

$$\vec{v_1} = \begin{bmatrix} \frac{C_q + \lambda}{D_q} \\ 1 \end{bmatrix} \tag{152}$$

$$\vec{v_2} = \begin{bmatrix} \frac{C_q - \lambda}{D_q} \\ 1 \end{bmatrix} \tag{153}$$

for λ and $-\lambda$ respectively. The Bogoliubov lengths are

$$\begin{aligned} l_1 &= \sqrt{\frac{(C_q+\lambda)^2}{D_q^2} - 1}, \\ l_2 &= \sqrt{1 - \frac{(C_q-\lambda)^2}{D_q^2}}, \end{aligned} \tag{154}$$

such that the Bogoliubov orthonormal vectors are

$$\vec{x_1} = \begin{bmatrix} \frac{C_q+\lambda}{D_q l_1} \\ \frac{1}{l_1} \end{bmatrix}, \tag{155}$$

$$\vec{x_2} = \begin{bmatrix} \frac{C_q-\lambda}{D_q l_2} \\ \frac{1}{l_2} \end{bmatrix}. \tag{156}$$

The transformation matrix is then

$$T = \begin{bmatrix} \vec{x_1} & \vec{x_2} \end{bmatrix} = \begin{bmatrix} \frac{C_q+\lambda}{D_q l_1} & \frac{C_q-\lambda}{D_q l_2} \\ \frac{1}{l_1} & \frac{1}{l_2} \end{bmatrix}. \tag{157}$$

Define the values

$$u_q = \frac{1}{l_2} = \frac{C_q+\lambda}{D_q l_1} = \sqrt{\frac{C_q+\lambda}{2\lambda}}, \tag{158}$$

$$v_q = \frac{1}{l_1} = \frac{C_q-\lambda}{D_q l_2} = \sqrt{\frac{C_q-\lambda}{2\lambda}}, \tag{159}$$

which satisfy the relationship

$$u_q^2 - v_q^2 = \frac{C_q+\lambda}{2\lambda} - \frac{C_q-\lambda}{2\lambda} = 1. \tag{160}$$

Furthermore, expanding these expressions, we find

$$\begin{aligned} u_q^2 &= \frac{1}{2}\left(\frac{\lambda}{\lambda} + \frac{C_q}{\lambda}\right) \\ &= \frac{1}{2}\Big(1 + \frac{C_q}{\sqrt{C_q^2 - D_q^2}}\Big) = \frac{1}{2}\Big(1 + \frac{1}{\sqrt{1 - D_q^2/C_q^2}}\Big). \end{aligned} \tag{161}$$

$$\begin{aligned} \frac{D_q}{C_q} &= \frac{S\Delta J\gamma(q)}{JSz - S\overline{J}\gamma(q)} \\ &= \frac{\Delta J\gamma(q)}{Jz - \overline{J}\gamma(q)}. \end{aligned} \tag{162}$$

$$\begin{aligned} 1 - \frac{D_q^2}{C_q^2} &= \frac{(Jz - \overline{J}\gamma)^2 - \Delta J^2\gamma^2(q)}{(Jz - \overline{J}\gamma(q))^2} \\ &= \frac{(Jz - \overline{J}\gamma(q) - \Delta J\gamma(q))(Jz - \overline{J}\gamma(q) + \Delta J\gamma(q)}{(Jz - \overline{J}\gamma(q))^2} \\ &= \frac{(Jz - J_x\gamma(q))(Jz - J_y\gamma(q))}{(Jz - \overline{J}\gamma(q))^2}. \end{aligned} \tag{163}$$

Inserting this into 161 gives

$$u_q^2 = \frac{1}{2}(1 + \frac{Jz - \overline{J}\gamma(q)}{\sqrt{(Jz - J_x\gamma(q))(Jz - J_y\gamma(q))}}) \tag{164}$$

and

$$v_q^2 = u_q^2 - 1 = \frac{1}{2}(-1 + \frac{Jz - \overline{J}\gamma(q)}{\sqrt{(Jz - J_x\gamma(q))(Jz - J_y\gamma(q))}}) \tag{165}$$

in terms of the system parameters.

Inserting equations 158 and 159 into the transformation matrix yields

$$T = \begin{bmatrix} u_q & v_q \\ v_q & u_q \end{bmatrix} \tag{166}$$

and

$$T^{-1} = \begin{bmatrix} u_q & -v_q \\ -v_q & u_q \end{bmatrix}. \tag{167}$$

Define the vectors of transformed operators

$$\vec{\phi}^\dagger = \begin{bmatrix} A_q^\dagger, & A_{-q} \end{bmatrix}, \tag{168}$$

$$\vec{\phi} = \begin{bmatrix} A_q \\ A_{-q}^\dagger \end{bmatrix} \tag{169}$$

By the Bogoliubov transformation, these are

$$\begin{bmatrix} A_q^\dagger, & A_{-q} \end{bmatrix} = \vec{\Phi}^\dagger T = \begin{bmatrix} u_q a_q^\dagger + v_q a_{-q}, & v_q a_q^\dagger + u_q a_{-q} \end{bmatrix} \tag{170}$$

$$\begin{bmatrix} A_q \\ A_{-q}^\dagger \end{bmatrix} = JT^{-1}J\vec{\Phi} = \begin{bmatrix} u_q a_q + v_q a_{-q}^\dagger \\ v_q a_q + u_q a_{-q}^\dagger \end{bmatrix} \tag{171}$$

with inverse transformations

$$\begin{bmatrix} a_q \\ a_{-q}^\dagger \end{bmatrix} = JTJ\vec{\phi} = \begin{bmatrix} u_q A_q - v_q A_{-q}^\dagger \\ -v_q A_q + u_q A_{-q}^\dagger \end{bmatrix}, \tag{172}$$

$$\begin{bmatrix} a_q^\dagger & a_{-q} \end{bmatrix} = \vec{\phi}^\dagger T^{-1} = \begin{bmatrix} u_q A_q^\dagger - v_q A_{-q}, & -v_q A_q^\dagger + u_q A_{-q} \end{bmatrix}. \tag{173}$$

The diagonal matrix is $D = diag(\lambda, \lambda)$, such that

$$H_{FM} = E_0^* + \sum_q \vec{\phi}^\dagger D \vec{\phi} = E_0^* + \sum_q \lambda\big(A_q^\dagger A_q + A_{-q} A_{-q}^\dagger\big)$$

$$= E_0^* + \sum_q \lambda(A_q^\dagger A_q + A_{-q}^\dagger A_{-q} + 1) = E_0^* + \sum_q 2\lambda\big(A_q^\dagger A_q + \frac{1}{2}\big)$$

Hence, the transformed ferromagnet Hamiltonian is

$$H_{FM} = E_0^* + \sum_q \omega_q (A_q^\dagger A_q + \frac{1}{2}), \tag{174}$$

where $E_0^* = -JNzS^2 - \sum_q C_q$ and $\omega_q = 2\sqrt{C_q^2 - D_q^2}$.

C Calculating coefficients for SW transformation in monolayer model

In the monolayer model, the perturbation is given by

$$H_1 = H_c = -V \sum_{k,q} \Big[u_q A_q c_{k+q,\downarrow}^\dagger c_{k,\uparrow} + u_q A_{-q}^\dagger c_{k+q,\uparrow}^\dagger c_{k,\downarrow} - v_q A_{-q}^\dagger c_{k+q,\downarrow}^\dagger c_{k,\uparrow} - v_q A_q c_{k+q,\uparrow}^\dagger c_{k,\downarrow} \Big], \tag{175}$$

and the generator by

$$S = -V \sum_{k,q} \Big[X_{kq} A_q c_{k+q,\downarrow}^\dagger c_{k\uparrow} + Y_{kq} A_{-q}^\dagger c_{k+q,\uparrow}^\dagger c_{k\downarrow} + Z_{kq} A_{-q}^\dagger c_{k+q,\downarrow}^\dagger c_{k\uparrow} + W_{kq} A_q c_{k+q,\uparrow}^\dagger c_{k\downarrow} \Big]. \tag{176}$$

From 2.3.3, the equation for the coefficients is

$$X_k = \frac{C_k}{E_m - E_n}. \tag{177}$$

All terms that contain a particle $\tilde{n}_{-q}$ uses the relation $\omega_{-q} = \omega_q$ to calculate the energy.

Start with the term with X_{kq} as coefficient. The operators are $A_q c^\dagger_{k+q,\downarrow} c_{k\uparrow}$. Thus $|m\rangle = |n_{k\uparrow}, n_{k+q,\downarrow}, \tilde{n}_q\rangle = |1,0,1\rangle$ and $|n\rangle = |0,1,0\rangle$. This gives

$$E_m - E_n = \varepsilon_{k\uparrow} - \varepsilon_{k+q,\downarrow} + \omega_q$$

From H_1, one has $C = u_q$, such that the coefficient is

$$X_{kq} = \frac{u_q}{\varepsilon_{k\uparrow} - \varepsilon_{k+q,\downarrow} + \omega_q} \tag{178}$$

Consider next the term with Y_{kq} as coefficient. Here the operators are $A^\dagger_{-q} c^\dagger_{k+q,\uparrow} c_{k\downarrow}$. Thus $|m\rangle = |n_{k\downarrow}, n_{k+q,\uparrow}, \tilde{n}_{-q}\rangle = |1,0,0\rangle$ and $|n\rangle = |0,1,1\rangle$, such that

$$E_m - E_n = \varepsilon_{k\downarrow} - \varepsilon_{k+q,\uparrow} - \omega_q.$$

From H_1, one has $C = u_q$, so the coefficient becomes

$$Y_{kq} = \frac{u_q}{\varepsilon_{k,\downarrow} - \varepsilon_{k+q,\uparrow} - \omega_q} \tag{179}$$

Consider next the term with Z_{kq} as coefficient. The operators are $A^\dagger_{-q} c^\dagger_{k+q,\downarrow} c_{k\uparrow}$, so the states are $|m\rangle = |n_{k\uparrow}, n_{k+q,\downarrow}, \tilde{n}_{-q}\rangle = |1,0,0\rangle$ and $|n\rangle = |0,1,1\rangle$. Thus

$$E_m - E_n = \varepsilon_{k\uparrow} - \varepsilon_{k+q,\downarrow} - \omega_q$$

From H_1, one has $C = -v_q$, such that

$$Z_{kq} = \frac{v_q}{\varepsilon_{k+q,\downarrow} - \varepsilon_{k\uparrow} + \omega_q} \tag{180}$$

Lastly, consider the term with W_{kq} as coefficient. The operators are $A_q c^\dagger_{k+q,\uparrow} c_{k\downarrow}$, so the states become $|m\rangle = |n_{k\downarrow}, n_{k+q,\uparrow}, \tilde{n}_q\rangle = |1,0,1\rangle$ and $|n\rangle = |0,1,0\rangle$. Thus

$$E_m - E_n = \varepsilon_{k\downarrow} - \varepsilon_{k+q,\uparrow} + \omega_q.$$

From H_1 one has $C = -v_q$, so the coefficient is

$$W_{kq} = \frac{v_q}{\varepsilon_{k+q,\uparrow} - \varepsilon_{k\downarrow} - \omega_q} \tag{181}$$

D Calculating SW transformation in monolayer model

In the monolayer model, the perturbation is given by

$$H_1 = H_c = -V \sum_{k,q} \Big[u_q A_q c^\dagger_{k+q,\downarrow} c_{k,\uparrow} + u_q A^\dagger_{-q} c^\dagger_{k+q,\uparrow} c_{k,\downarrow} - v_q A^\dagger_{-q} c^\dagger_{k+q,\downarrow} c_{k,\uparrow} - v_q A_q c^\dagger_{k+q,\uparrow} c_{k,\downarrow} \Big], \tag{182}$$

and the generator by

$$S = -V \sum_{k,q} \Big[X_{kq} A_q c^\dagger_{k+q,\downarrow} c_{k\uparrow} + Y_{kq} A^\dagger_{-q} c^\dagger_{k+q,\uparrow} c_{k\downarrow} + Z_{kq} A^\dagger_{-q} c^\dagger_{k+q,\downarrow} c_{k\uparrow} + W_{kq} A_q c^\dagger_{k+q,\uparrow} c_{k\downarrow} \Big]. \tag{183}$$

In this section, the commutator $-\frac{1}{2}[S, H_1]$ is calculated.

To more easily calculate the commutator, the calculation can be performed in general first, and then applied to the relevant terms. Let a and b be operators representing magnons, and let A and B be two fermionic operators each. Then

$$\begin{aligned}[aA, bB] &= aAbB - bBaA = abAB - baBA \\ &= abAB + (-baAB + baAB) - baBA \\ &= (ab - ba)AB + ba(AB - BA) \\ &= [a, b]AB + ba[A, B]\end{aligned}$$

In this case, the terms of the form $ba[A, B]$ are not used, so discard these. Then we have $[aA, bB] = [a, b]AB$. Note that if $a = A_q$, $b = A_{q'}$ or $a = A^\dagger_{-q}$, $b = A^\dagger_{-q'}$ then $[a, b] = 0$. If $a = A_q$, $b = A^\dagger_{-q'}$ then $[a, b] = \delta_{q',-q}$, and if $a = A^\dagger_{-q}$, $b = A_{q'}$, then $[a, b] = -\delta_{q',-q}$. This covers all possible cases in this commutator. Let a and A be the operators in S and let b and B be the operators in H_1. Thus, the fermionic anticommutation relation is treated as $\{c^\dagger_\lambda, c_{\lambda'}\} = 0$.

By the bilinearity of commutators, the commutator can be calculated term-by-term by commuting the terms with each other. There are then eight terms to calculate. Pair the first term of S with the second and third terms of H_1 and calculate their commutator to get

$$-\delta_{q',-q} X_{kq} V^2 v_{q'} c^\dagger_{k+q,\downarrow} c_{k\uparrow} c^\dagger_{k'+q',\downarrow} c_{k'\uparrow} + \delta_{q',-q} X_{kq} V^2 u_{q'} c^\dagger_{k+q,\downarrow} c_{k\uparrow} c^\dagger_{k'+q',\uparrow} c_{k'\downarrow}. \tag{184}$$

Pair the second term of S with the first and fourth terms of H_1 to get

$$-\delta_{q',-q} Y_{kq} V^2 u_{q'} c^\dagger_{k+q,\uparrow} c_{k\downarrow} c^\dagger_{k'+q',\downarrow} c_{k'\uparrow} + \delta_{q',-q} Y_{kq} V^2 v_{q'} c^\dagger_{k+q,\uparrow} c_{k\downarrow} c^\dagger_{k'+q',\uparrow} c_{k'\downarrow}. \tag{185}$$

Pair the third term of S with the first and fourth terms of H_1 to get

$$-\delta_{q',-q} Z_{kq} V^2 u_{q'} c^\dagger_{k+q,\downarrow} c_{k\uparrow} c^\dagger_{k'+q',\downarrow} c_{k'\uparrow} + \delta_{q',-q} Z_{kq} V^2 v_{q'} c^\dagger_{k+q,\downarrow} c_{k\uparrow} c^\dagger_{k'+q',\uparrow} c_{k'\downarrow}. \tag{186}$$

Lastly, pair the fourth term of S with the second and third terms of H_1 to get

$$-\delta_{q',-q} W_{kq} V^2 v_{q'} c^\dagger_{k+q,\uparrow} c_{k\downarrow} c^\dagger_{k'+q',\downarrow} c_{k'\uparrow} + \delta_{q',-q} W_{kq} V^2 u_{q'} c^\dagger_{k+q,\uparrow} c_{k\downarrow} c^\dagger_{k'+q',\uparrow} c_{k'\downarrow} \tag{187}$$

Collect all terms and sum over all the variables:

$$\begin{aligned}-\frac{1}{2}[S, H_1] = -\frac{V^2}{2} \sum_{k,k',q,q'} \Big[&- \delta_{q',-q} X_{kq} v_{q'} c^\dagger_{k+q,\downarrow} c_{k\uparrow} c^\dagger_{k'+q',\downarrow} c_{k'\uparrow} + \delta_{q',-q} X_{kq} u_{q'} c^\dagger_{k+q,\downarrow} c_{k\uparrow} c^\dagger_{k'+q',\uparrow} c_{k'\downarrow} \\ &- \delta_{q',-q} Y_{kq} u_{q'} c^\dagger_{k+q,\uparrow} c_{k\downarrow} c^\dagger_{k'+q',\downarrow} c_{k'\uparrow} + \delta_{q',-q} Y_{kq} v_{q'} c^\dagger_{k+q,\uparrow} c_{k\downarrow} c^\dagger_{k'+q',\uparrow} c_{k'\downarrow} \\ &- \delta_{q',-q} Z_{kq} u_{q'} c^\dagger_{k+q,\downarrow} c_{k\uparrow} c^\dagger_{k'+q',\downarrow} c_{k'\uparrow} + \delta_{q',-q} Z_{kq} v_{q'} c^\dagger_{k+q,\downarrow} c_{k\uparrow} c^\dagger_{k'+q',\uparrow} c_{k'\downarrow} \\ &- \delta_{q',-q} W_{kq} v_{q'} c^\dagger_{k+q,\uparrow} c_{k\downarrow} c^\dagger_{k'+q',\downarrow} c_{k'\uparrow} + \delta_{q',-q} W_{kq} u_{q'} c^\dagger_{k+q,\uparrow} c_{k\downarrow} c^\dagger_{k'+q',\uparrow} c_{k'\downarrow} \Big]\end{aligned} \tag{188}$$

Gather all terms with similar spin structure in the fermionic operators and use the fact that $u_{-q} = u_q$ and $v_{-q} = v_q$ to get

$$\begin{aligned}-\frac{1}{2}[S, H_1] = &-\frac{V^2}{2} \sum_{k,k',q} \Big[X_{kq} u_q c^\dagger_{k+q,\downarrow} c_{k\uparrow} c^\dagger_{k'-q,\uparrow} c_{k'\downarrow} - Y_{kq} u_q c^\dagger_{k+q,\uparrow} c_{k\downarrow} c^\dagger_{k'-q,\downarrow} c_{k'\uparrow} \\ &\qquad + Z_{kq} v_q c^\dagger_{k+q,\downarrow} c_{k\uparrow} c^\dagger_{k'-q,\uparrow} c_{k'\downarrow} - W_{kq} v_q c^\dagger_{k+q,\uparrow} c_{k\downarrow} c^\dagger_{k'-q,\downarrow} c_{k'\uparrow} \Big] \\ &-\frac{V^2}{2} \sum_{k,k',q} \Big[Y_{kq} v_q c^\dagger_{k+q,\uparrow} c_{k\downarrow} c^\dagger_{k'-q,\uparrow} c_{k'\downarrow} + W_{kq} u_q c^\dagger_{k+q,\uparrow} c_{k\downarrow} c^\dagger_{k'-q,\uparrow} c_{k'\downarrow} \Big] \\ &+\frac{V^2}{2} \sum_{k,k',q} \Big[X_{kq} v_q c^\dagger_{k+q,\downarrow} c_{k\uparrow} c^\dagger_{k'-q,\downarrow} c_{k'\uparrow} + Z_{kq} u_q c^\dagger_{k+q,\downarrow} c_{k\uparrow} c^\dagger_{k'-q,\downarrow} c_{k'\uparrow} \Big]\end{aligned} \tag{189}$$

Consider the first sum first. In the second and fourth terms exchange $\vec{k}$ and $\vec{k}'$ and let $\vec{q} \to -\vec{q}$ to get

$$-\frac{V^2}{2}\sum_{k,k',q}\Big[X_{kq}u_q c^\dagger_{k+q,\downarrow}c_{k\uparrow}c^\dagger_{k'-q,\uparrow}c_{k'\downarrow} - Y_{k',-q}u_q c^\dagger_{k'-q,\uparrow}c_{k'\downarrow}c^\dagger_{k+q,\downarrow}c_{k\uparrow} \\ Z_{kq}v_q c^\dagger_{k+q,\downarrow}c_{k\uparrow}c^\dagger_{k'-q,\uparrow}c_{k'\downarrow} - W_{k',-q}v_q c^\dagger_{k'-q,\uparrow}c_{k'\downarrow}c^\dagger_{k+q,\downarrow}c_{k\uparrow}\Big] \tag{190}$$

In these terms, anticommute $c^\dagger_{k+q,\uparrow}c_{k\downarrow}$ to the front and ignore all extra terms that arise from the anticommutation. The result is

$$\sum_{k,k',q}\Big[\underbrace{\frac{V^2}{2}\big(Y_{k',-q}u_q + W_{k',-q}v_q - X_{kq}u_q - Z_{kq}v_q\big)}_{\mathrm{V}^{opposite}_{eff}} c^\dagger_{k+q,\downarrow}c_{k\uparrow}c^\dagger_{k'-q,\uparrow}c_{k'\downarrow}\Big] \tag{191}$$

Consider next the second sum. In the first term, exchange $\vec{k}$ and $\vec{k}'$ and let $\vec{q} \to -\vec{q}$ to get

$$-\frac{V^2}{2}\sum_{k,k',q}\Big[Y_{k',-q}v_q c^\dagger_{k'-q,\uparrow}c_{k'\downarrow}c^\dagger_{k+q,\uparrow}c_{k\downarrow} + W_{kq}u_q c^\dagger_{k+q,\uparrow}c_{k\downarrow}c^\dagger_{k'-q,\uparrow}c_{k'\downarrow}\Big] \tag{192}$$

Anticommute $c^\dagger_{k+q,\uparrow}c_{k\downarrow}$ to the front to get

$$\sum_{k,k',q}\Big[\underbrace{-\frac{V^2}{2}\big(Y_{k',-q}v_q + W_{kq}u_q\big)}_{\mathrm{V}^{up}_{eff}} c^\dagger_{k+q,\uparrow}c_{k\downarrow}c^\dagger_{k'-q,\uparrow}c_{k'\downarrow}\Big] \tag{193}$$

In the third sum exchange $\vec{k}$ and $\vec{k}'$ as well as letting $\vec{q} \to -\vec{q}$ in the second term and anticommute $c^\dagger_{k+q,\downarrow}c_{k\uparrow}$ to the front to get

$$\sum_{k,k',q}\Big[\underbrace{\frac{V^2}{2}\big(X_{kq}v_q + Z_{k',-q}u_q\big)}_{\mathrm{V}^{down}_{eff}} c^\dagger_{k+q,\downarrow}c_{k\uparrow}c^\dagger_{k'-q,\downarrow}c_{k'\uparrow}\Big]. \tag{194}$$

In total, this gives the commutator as

$$-\frac{1}{2}[S,H_1] = \sum_{k,k',q}\Big[V^{opposite}_{eff}c^\dagger_{k+q,\downarrow}c_{k\uparrow}c^\dagger_{k'-q,\uparrow}c_{k'\downarrow} + V^{up}_{eff}c^\dagger_{k+q,\uparrow}c_{k\downarrow}c^\dagger_{k'-q,\uparrow}c_{k'\downarrow} + V^{down}_{eff}c^\dagger_{k+q,\downarrow}c_{k\uparrow}c^\dagger_{k'-q,\downarrow}c_{k'\uparrow}\Big]. \tag{195}$$

Anticommute all creation operators to the left to get the commutator

$$-\frac{1}{2}[S,H_1] = -\sum_{k,k',q}\Big[V^{opposite}_{eff}c^\dagger_{k+q,\downarrow}c^\dagger_{k'-q,\uparrow}c_{k\uparrow}c_{k'\downarrow} + V^{up}_{eff}c^\dagger_{k+q,\uparrow}c^\dagger_{k'-q,\uparrow}c_{k\downarrow}c_{k'\downarrow} + V^{down}_{eff}c^\dagger_{k+q,\downarrow}c^\dagger_{k'-q,\downarrow}c_{k\uparrow}c_{k'\uparrow}\Big]. \tag{196}$$

E BCS reduction, monolayer model

The BCS reduction is performed by first considering the interactions, inserting the BCS reduction and then rewriting every term before combining and simplifying the expressions. The index changes are $\vec{k}' \to -\vec{k}$, then defining $\vec{q} = \vec{k}' - \vec{k}$ and lastly exchanging $\vec{k}$ and $\vec{k}'$.

From equations 75, 76 and 77 the interactions are as

$$V^{opposite}_{eff} = -\frac{V^2}{2}\big(X_{kq}u_q + Z_{kq}v_q - Y_{k',-q}u_q - W_{k',-q}v_q\big), \tag{197}$$

$$V^{up}_{eff} = -\frac{V^2}{2}\big(Y_{k',-q}v_q + W_{kq}u_q\big), \tag{198}$$

$$V_{eff}^{down} = \frac{V^2}{2}\big(X_{kq}v_q + Z_{k',-q}u_q\big) \tag{199}$$

Inserting the variable changes, the BCS-interactions become

$$V_{kk'}^{opposite} = -\frac{V^2}{2}\big(X_{k',k-k'}u_{k-k'} + Z_{k',k-k'q}v_{k-k'} - Y_{-k',k'-k}u_{k-k'} - W_{-k',k'-k}v_{k-k'}\big), \tag{200}$$

$$V_{kk'}^{up} = -\frac{V^2}{2}\big(Y_{-k',k'-k}v_{k-k'} + W_{k',k-k'}u_{k-k'}\big), \tag{201}$$

$$V_{kk'}^{down} = \frac{V^2}{2}\big(X_{k',k-k'}v_{k-k'} + Z_{-k',k'-k}u_{k-k'}\big) \tag{202}$$

To proceed, rewrite every coefficient. The fermion energies are given by

$$\varepsilon_{k\sigma} = \varepsilon_k - \sigma m, \tag{203}$$

where

$$\varepsilon_k = -t\gamma(\vec{k}) - \mu, \tag{204}$$

$$m = h + SJ_{sd}. \tag{205}$$

Also define the offset magnon energies given by

$$\tilde{\omega}_q^{\pm} = \omega_q \pm 2m. \tag{206}$$

The spin is defined as $\sigma = 1$ for spin up and $\sigma = -1$ for spin down. One can then write X_{kq} as

$$\begin{aligned} X_{kq} = \frac{u_q}{\varepsilon_{k\uparrow} - \varepsilon_{k+q,\downarrow} + \omega_q} &= \frac{u_q}{\varepsilon_k - m - \varepsilon_{k+q} - m + \omega_q} \\ &= \frac{u_q}{(\varepsilon_k - \varepsilon_{k+q}) + \tilde{\omega}_q^-} \end{aligned} \tag{207}$$

Doing the same for Y_{kq} one gets

$$\begin{aligned} Y_{kq} = \frac{u_q}{\varepsilon_{k\downarrow} - \varepsilon_{k+q,\uparrow} - \omega_q} &= \frac{u_q}{\varepsilon_k + m - \varepsilon_{k+q} + m - \omega_q} \\ &= \frac{u_q}{(\varepsilon_k - \varepsilon_{k+q}) - \tilde{\omega}_q^-} \end{aligned} \tag{208}$$

For Z_{kq} one gets

$$\begin{aligned} Z_{kq} = \frac{v_q}{\varepsilon_{k+q,\downarrow} - \varepsilon_{k\uparrow} + \omega_q} &= \frac{v_q}{\varepsilon_{k+q} + m - \varepsilon_k + m + \omega_q} \\ &= \frac{v_q}{(\varepsilon_{k+q} - \varepsilon_k) + \tilde{\omega}_q^+} \end{aligned} \tag{209}$$

And W_{kq} becomes

$$\begin{aligned} W_{kq} = \frac{v_q}{\varepsilon_{k+q,\uparrow} - \varepsilon_{k\downarrow} - \omega_q} &= \frac{v_q}{\varepsilon_{k+q} - m - \varepsilon_k - m - \omega_q} \\ &= \frac{v_q}{(\varepsilon_{k+q} - \varepsilon_k) - \tilde{\omega}_q^+} \end{aligned} \tag{210}$$

Starting with the expression for $V_{kk'}^{opposite}$, inserting the reduced coefficients gives

$$\begin{aligned} V_{kk'}^{opposite} = -\frac{V^2}{2}\Big(&\frac{u_{k-k'}^2}{(\varepsilon_{k'} - \varepsilon_k) + \tilde{\omega}_{k-k'}^-} - \frac{u_{k-k'}^2}{(\varepsilon_{k'} - \varepsilon_k) - \tilde{\omega}_{k-k'}^-} \\ &+ \frac{v_{k-k'}^2}{(\varepsilon_k - \varepsilon_{k'}) + \tilde{\omega}_{k-k'}^+} - \frac{v_{k-k'}^2}{(\varepsilon_k - \varepsilon_{k'}) - \tilde{\omega}_{k-k'}^+}\Big) \end{aligned}$$

which can be simplified further

$$V_{kk'}^{opposite} = -\frac{V^2}{2}\Big(\frac{u_{k-k'}^2\big((\varepsilon_{k'}-\varepsilon_k)-\tilde{\omega}_{k-k'}^{-}-(\varepsilon_{k'}-\varepsilon_k)-\tilde{\omega}_{k-k'}^{-}\big)}{(\varepsilon_{k'}-\varepsilon_k)^2-(\tilde{\omega}_{k-k'}^{-})^2}+\frac{v_{k-k'}^2\big((\varepsilon_k-\varepsilon_{k'})-\tilde{\omega}_{k-k'}^{+}-(\varepsilon_k-\varepsilon_{k'})-\tilde{\omega}_{k-k'}^{+}\big)}{(\varepsilon_k-\varepsilon_{k'})^2-(\tilde{\omega}_{k-k'}^{+})^2}\Big)$$

$$V_{kk'}^{opposite} = \frac{V^2u_{k-k'}^2\tilde{\omega}_{k-k'}^{-}}{(\varepsilon_k-\varepsilon_{k'})^2-(\tilde{\omega}_{k-k'}^{-})^2}+\frac{V^2v_{k-k'}^2\tilde{\omega}_{k-k'}^{+}}{(\varepsilon_k-\varepsilon_{k'})^2-(\tilde{\omega}_{k-k'}^{+})^2} \tag{211}$$

Performing the same procedure for $V_{kk'}^{up}$, one gets

$$V_{kk'}^{up} = -\frac{V^2}{2}\Big(\frac{u_{k-k'}v_{k-k'}}{(\varepsilon_{k'}-\varepsilon_k)-\tilde{\omega}_{k-k'}^{-}}-\frac{u_{k-k'}v_{k-k'}}{(\varepsilon_{k'}-\varepsilon_k)+\tilde{\omega}_{k-k'}^{+}}\Big)$$

which can be simplified as

$$V_{kk'}^{up} = -\frac{V^2}{2}\frac{u_{k-k'}v_{k-k'}\big((\varepsilon_{k'}-\varepsilon_k)+\tilde{\omega}_{k-k'}^{+}-(\varepsilon_{k'}-\varepsilon_k)+\tilde{\omega}_{k-k'}^{-}\big)}{\big((\varepsilon_{k'}-\varepsilon_k)-\tilde{\omega}_{k-k'}^{-}\big)\big((\varepsilon_{k'}-\varepsilon_k)+\tilde{\omega}_{k-k'}^{+}\big)}$$

$$V_{kk'}^{up} = -\frac{V^2u_{k-k'}v_{k-k'}\omega_{k-k'}}{(\varepsilon_k-\varepsilon_{k'})^2-(\tilde{\omega}_{k-k'}^{+}-\tilde{\omega}_{k-k'})(\varepsilon_k-\varepsilon_{k'})-\tilde{\omega}_{k-k'}^{+}\tilde{\omega}_{k-k'}^{-}} \tag{212}$$

Similarly, for $V_{kk'}^{down}$ one gets

$$V_{kk'}^{down} = \frac{V^2}{2}\Big(\frac{u_{k-k'}v_{k-k'}}{(\varepsilon_{k'}-\varepsilon_k)+\tilde{\omega}_{k-k'}^{-}}-\frac{u_{k-k'}v_{k-k'}}{(\varepsilon_{k'}-\varepsilon_k)-\tilde{\omega}_{k-k'}^{+}}\Big)$$

which simplifies to

$$V_{kk'}^{down} = \frac{V^2}{2}\frac{u_{k-k'}v_{k-k'}\big((\varepsilon_{k'}-\varepsilon_k)-\tilde{\omega}_{k-k'}^{+}-(\varepsilon_{k'}-\varepsilon_k)-\tilde{\omega}_{k-k'}^{-}\big)}{\big((\varepsilon_{k'}-\varepsilon_k)+\tilde{\omega}_{k-k'}^{-}\big)\big((\varepsilon_{k'}-\varepsilon_k)-\tilde{\omega}_{k-k'}^{+}\big)}$$

$$V_{kk'}^{down} = -\frac{V^2u_{k-k'}v_{k-k'}\omega_{k-k'}}{(\varepsilon_k-\varepsilon_{k'})^2+(\tilde{\omega}_{k-k'}^{+}-\tilde{\omega}_{k-k'})(\varepsilon_k-\varepsilon_{k'})-\tilde{\omega}_{k-k'}^{+}\tilde{\omega}_{k-k'}^{-}} \tag{213}$$

F Bogoliubov transformation of H_{FM} in two-layer model

In the two-layer model, the FMI-Hamiltonian is given by

$$H = E_0^* + \sum_q \begin{bmatrix} a_q^\dagger, & b_q^\dagger, & a_{-q} & b_{-q}\end{bmatrix}\begin{bmatrix} C_q+\Delta & -\Delta & D_q & 0\\ -\Delta & C_q+\Delta & 0 & D_q\\ D_q & 0 & C_q+\Delta & -\Delta\\ 0 & D_q & -\Delta & C_q+\Delta\end{bmatrix}\begin{bmatrix} a_q\\ b_q\\ a_{-q}^\dagger\\ b_{-q}^\dagger\end{bmatrix}, \tag{214}$$

where $E_0^* = -2JNzS^2 - J_pNS^2 - 2\sum_q C_q - 2N\Delta$. This section follows the same procedure as in appendix B. The eigenvalues of PJ are

$$\lambda_{1\pm} = \pm\lambda_1 = \pm\sqrt{C_q^2-D_q^2}, \tag{215}$$

$$\lambda_{2\pm} = \pm\lambda_2 = \pm\sqrt{(C_q+2\Delta)^2-D_q^2}. \tag{216}$$

and the corresponding eigenvectors are

$$\vec{v}_1 = \begin{bmatrix}\frac{C_q+\lambda_1}{D_q}\\ \frac{C_q+\lambda_1}{D_q}\\ 1\\ 1\end{bmatrix} \tag{217}$$

$$\vec{v}_2 = \begin{bmatrix} -\frac{C_q+2\Delta+\lambda_2}{D_q} \\ \frac{C_q+2\Delta+\lambda_2}{D_q} \\ -1 \\ 1 \end{bmatrix} \tag{218}$$

$$\vec{v}_3 = \begin{bmatrix} \frac{C_q-\lambda_1}{D_q} \\ \frac{C_q-\lambda_1}{D_q} \\ 1 \\ 1 \end{bmatrix} \tag{219}$$

$$\vec{v}_4 = \begin{bmatrix} -\frac{C_q+2\Delta-\lambda_2}{D_q} \\ \frac{C_q+2\Delta-\lambda_2}{D_q} \\ -1 \\ 1 \end{bmatrix} \tag{220}$$

Define next the Bogoliubov lengths of the four eigenvectors of PJ

$$l_1 = \sqrt{2\frac{(C_q+\lambda_1)^2}{D_q^2} - 2}, \tag{221}$$

$$l_2 = \sqrt{2\frac{(C_q+2\Delta+\lambda_2)^2}{D_q^2} - 2}, \tag{222}$$

$$l_3 = \sqrt{2 - 2\frac{(C_q-\lambda_1)^2}{D_q^2}}, \tag{223}$$

$$l_4 = \sqrt{2 - 2\frac{(C_q+2\Delta-\lambda_2)^2}{D_q^2}}, \tag{224}$$

as well as the values

$$u_{q1} = \frac{1}{l_3} = \frac{1}{2}\sqrt{\frac{C_q+\lambda_1}{\lambda_1}}, \tag{225}$$

$$u_{q2} = \frac{1}{l_4} = \frac{1}{2}\sqrt{\frac{C_q+2\Delta+\lambda_2}{\lambda_2}}, \tag{226}$$

$$v_{q1} = \frac{1}{l_1} = \frac{1}{2}\sqrt{\frac{C_q-\lambda_1}{\lambda_1}}, \tag{227}$$

$$v_{q2} = \frac{1}{l_2} = \frac{1}{2}\sqrt{\frac{C_q+2\Delta-\lambda_2}{\lambda_2}} \tag{228}$$

which satisfy the relationships

$$\begin{aligned} u_{q1}^2 - v_{q1}^2 &= \frac{1}{2}, \\ u_{q2}^2 - v_{q2}^2 &= \frac{1}{2}, \\ (u_{q1}^2 + u_{q2}^2) - (v_{q1}^2 + v_{q2}^2) &= 1. \end{aligned} \tag{229}$$

The Bogoliubov orthonormalized eigenvectors are then

$$\vec{x}_1^T = \begin{bmatrix} u_{q1} & u_{q1} & v_{q1} & v_{q1} \end{bmatrix}, \tag{230}$$

$$\vec{x}_2^T = \begin{bmatrix} -u_{q2} & u_{q2} & -v_{q2} & v_{q2} \end{bmatrix}, \tag{231}$$

$$\vec{x}_3^T = \begin{bmatrix} v_{q1} & v_{q1} & u_{q1} & u_{q1} \end{bmatrix}, \tag{232}$$

$$\vec{x}_4^T = \begin{bmatrix} -v_{q2} & v_{q2} & -u_{q2} & u_{q2} \end{bmatrix}, \tag{233}$$

such that the transformation matrix becomes

$$T = \begin{bmatrix} \vec{x}_1 & \vec{x}_2 & \vec{x}_3 & \vec{x}_4 \end{bmatrix} = \begin{bmatrix} u_{q1} & -u_{q2} & v_{q1} & -v_{q2} \\ u_{q1} & u_{q2} & v_{q1} & v_{q2} \\ v_{q1} & -v_{q2} & u_{q1} & -u_{q2} \\ v_{q1} & v_{q2} & u_{q1} & u_{q2} \end{bmatrix}, \tag{234}$$

and its inverse is

$$T^{-1} = \begin{bmatrix} u_{q1} & u_{q1} & -v_{q1} & -v_{q1} \\ -u_{q2} & u_{q2} & v_{q2} & -v_{q2} \\ -v_{q1} & -v_{q1} & u_{q1} & u_{q1} \\ v_{q2} & -v_{q2} & -u_{q2} & u_{q2} \end{bmatrix} \tag{235}$$

Define the vector of operators representing long-lived magnons as

$$\vec{\phi}^\dagger = \begin{bmatrix} A_q^\dagger, & B_q^\dagger, & A_{-q}, & B_{-q} \end{bmatrix}. \tag{236}$$

The Bogoliubov transform then becomes

$$\vec{\phi}^* = \begin{bmatrix} A_q^\dagger \\ B_q^\dagger \\ A_{-q} \\ B_{-q} \end{bmatrix} = (\vec{\Phi}^\dagger T)^T = \begin{bmatrix} u_{q1}a_q^\dagger + u_{q1}b_q^\dagger + v_{q1}a_{-q} + v_{q1}b_{-q} \\ -u_{q2}a_q^\dagger + u_{q2}b_q^\dagger - v_{q2}a_{-q} + v_{q2}b_{-q} \\ v_{q1}a_q^\dagger + v_{q1}b_q^\dagger + u_{q1}a_{-q} + u_{q1}b_{-q} \\ -v_{q2}a_q^\dagger + v_{q2}b_q^\dagger - u_{q2}a_{-q} + u_{q2}b_{-q} \end{bmatrix}, \tag{237}$$

$$\vec{\phi} = \begin{bmatrix} A_q \\ B_q \\ A_{-q}^\dagger \\ B_{-q}^\dagger \end{bmatrix} = JT^{-1}J\vec{\Phi} = \begin{bmatrix} u_{q1}a_q + u_{q1}b_q + v_{q1}a_{-q}^\dagger + v_{q1}b_{-q}^\dagger \\ -u_{q2}a_q + u_{q2}b_q - v_{q2}a_{-q}^\dagger + v_{q2}b_{-q}^\dagger \\ v_{q1}a_q + v_{q1}b_q + u_{q1}a_{-q}^\dagger + u_{q1}b_{-q}^\dagger \\ -v_{q2}a_q + v_{q2}b_q - u_{q2}a_{-q}^\dagger + u_{q2}b_{-q}^\dagger \end{bmatrix}, \tag{238}$$

with diagonal matrix

$$D = \begin{bmatrix} \lambda_1 & 0 & 0 & 0 \\ 0 & \lambda_2 & 0 & 0 \\ 0 & 0 & \lambda_1 & 0 \\ 0 & 0 & 0 & \lambda_2 \end{bmatrix}. \tag{239}$$

The Hamiltonian thus becomes

$$\begin{aligned} H &= E_0^* + \sum_q \Big[\lambda_1\big(A_q^\dagger A_q + A_{-q}A_{-q}^\dagger\big) + \lambda_2\big(B_q^\dagger B_q + B_{-q}B_{-q}^\dagger\big)\Big] \\ &= E_0^* + \sum_q \Big[\lambda_1\big(A_q^\dagger A_q + A_{-q}^\dagger A_{-q} + 1\big) + \lambda_2\big(B_q^\dagger B_q + B_{-q}^\dagger B_{-q} + 1\big)\Big] \\ &= E_0^* + \sum_q \Big[2\lambda_1\big(A_q^\dagger A_q + \frac{1}{2}\big) + 2\lambda_2\big(B_q^\dagger B_q + \frac{1}{2}\big)\Big]. \end{aligned}$$

Define the values $\omega_{qi} = 2\lambda_i$, such that

$$H = E_0^* + \sum_{q,i} \omega_{qi}\big((A_q^i)^\dagger A_q^i + \frac{1}{2}\big), \tag{240}$$

with $A_q^1 = A_q$, $A_q^2 = B_q$ and $E_0^* = -2JNzS^2 - J_pNS^2 - 2\sum_q C_q - 2N\Delta$.

The required inverse transformation is given by

$$\begin{bmatrix} a_q \\ a_{-q}^\dagger \end{bmatrix} = \begin{bmatrix} u_{q1}A_q - u_{q2}B_q - v_{q1}A_{-q}^\dagger + v_{q2}B_{-q}^\dagger \\ -v_{q1}A_q + v_{q2}B_q + u_{q1}A_{-q}^\dagger - u_{q2}B_{-q}^\dagger \end{bmatrix}. \tag{241}$$

G Determining coefficients for SW transformation in two-layer model

In the two-layer model, the perturbation is given by

$$H_1 = H_c = -V\sum_{k,q,i}(-1)^{i+1}\Big[u_{qi}A_q^i c_{k+q,\downarrow}^\dagger c_{k\uparrow} - v_{qi}(A_{-q}^i)^\dagger c_{k+q,\downarrow}^\dagger c_{k\uparrow} + u_{qi}(A_{-q}^i)^\dagger c_{k+q,\uparrow}^\dagger c_{k\downarrow} - v_{qi}A_q^i c_{k+q,\uparrow}^\dagger c_{k\downarrow}\Big], \tag{242}$$

and the generator by

$$S = -V \sum_{k,q,i} (-1)^{i+1} \Big[X^i_{kq} A^i_q c^\dagger_{k+q,\downarrow} c_{k\uparrow} + Y^i_{kq} (A^i_{-q})^\dagger c^\dagger_{k+q,\uparrow} c_{k\downarrow} + Z^i_{kq} (A^i_{-q})^\dagger c^\dagger_{k+q,\downarrow} c_{k\uparrow} + W^i_{kq} A^i_q c^\dagger_{k+q,\uparrow} c_{k\downarrow} \Big]. \tag{243}$$

The equation used to determine the coefficients is

$$X_k = \frac{C_k}{E_m - E_n}. \tag{244}$$

Consider first X^i_{kq}. The operators are $A^i_q c^\dagger_{k+q,\downarrow} c_{k\uparrow}$. The states are $|m\rangle = |n_{k+q,\downarrow}, n_{k\uparrow}, \tilde{n}_{qi}\rangle = |0,1,1\rangle$ and $|n\rangle = |1,0,0\rangle$. Then

$$E_m - E_n = \varepsilon_{k\uparrow} - \varepsilon_{k+q,\downarrow} + \omega_{qi}, \tag{245}$$

and $C = u_{qi}$, such that the coefficient is

$$X^i_{kq} = \frac{u_{qi}}{\varepsilon_{k\uparrow} - \varepsilon_{k+q,\downarrow} + \omega_{qi}}. \tag{246}$$

Consider next Y^i_{kq}. It is the coefficient of the operators $(A^i_{-q})^\dagger c^\dagger_{k+q,\uparrow} c_{k\downarrow}$, so the states are $|m\rangle = |n_{k+q,\uparrow}, n_{k\downarrow}, \tilde{n}_{qi}\rangle = |0,1,0\rangle$ and $|n\rangle = |1,0,1\rangle$. The energies become

$$E_m - E_n = \varepsilon_{k\downarrow} - \varepsilon_{k+q,\uparrow} - \omega_{qi}, \tag{247}$$

and $C = u_{qi}$, such that the coefficient is

$$Y^i_{kq} = \frac{u_{qi}}{\varepsilon_{k\downarrow} - \varepsilon_{k+q,\uparrow} - \omega_{qi}}. \tag{248}$$

Consider next Z^i_{kq}, with operators $(A^i_{-q})^\dagger c^\dagger_{k+q,\downarrow} c_{k\uparrow}$. The states are $|m\rangle = |n_{k+q,\downarrow}, n_{k\uparrow}, \tilde{n}_{qi}\rangle = |0,1,0\rangle$ and $|n\rangle = |1,0,1\rangle$. The energies become

$$E_m - E_n = \varepsilon_{k\uparrow} - \varepsilon_{k+q,\downarrow} - \omega_{qi}, \tag{249}$$

and $C = -v_{qi}$, such that the coefficient is

$$Z^i_{kq} = \frac{v_{qi}}{\varepsilon_{k+q,\downarrow} - \varepsilon_{k,\uparrow} + \omega_{qi}}. \tag{250}$$

Lastly, consider W^i_{kq} with operators $A^i_q c^\dagger_{k+q,\uparrow} c_{k\downarrow}$. The states are $|m\rangle = |n_{k+q,\uparrow}, n_{k\downarrow}, \tilde{n}_{qi}\rangle = |0,1,1\rangle$ and $|n\rangle = |1,0,0\rangle$. Then

$$E_m - E_n = \varepsilon_{k\downarrow} - \varepsilon_{k+q,\uparrow} + \omega_{qi}, \tag{251}$$

and $C = -v_{qi}$, such that the coefficient is

$$W^i_{kq} = \frac{v_{qi}}{\varepsilon_{k+q,\uparrow} - \varepsilon_{k,\downarrow} - \omega_{qi}}. \tag{252}$$

H SW transformation, two-layer model

The perturbation is given by

$$H_1 = -V \sum_{k,q,i} (-1)^{i+1} \Big[u_{qi} A^i_q c^\dagger_{k+q,\downarrow} c_{k\uparrow} - v_{qi} (A^i_{-q})^\dagger c^\dagger_{k+q,\downarrow} c_{k\uparrow} + u_{qi} (A^i_{-q})^\dagger c^\dagger_{k+q,\uparrow} c_{k\downarrow} - v_{qi} A^i_q c^\dagger_{k+q,\uparrow} c_{k\downarrow} \Big], \tag{253}$$

and the generator by

$$S = -V \sum_{k,q,i} (-1)^{i+1} \Big[X^i_{kq} A^i_q c^\dagger_{k+q,\downarrow} c_{k\uparrow} + Y^i_{kq} (A^i_{-q})^\dagger c^\dagger_{k+q,\uparrow} c_{k\downarrow} + Z^i_{kq} (A^i_{-q})^\dagger c^\dagger_{k+q,\downarrow} c_{k\uparrow} + W^i_{kq} A^i_q c^\dagger_{k+q,\uparrow} c_{k\downarrow} \Big]. \tag{254}$$

These calculations follow the same rules as presented in appendix D. Furthermore, there are no crossterms since $[A_q^i, (A_q^j)^\dagger] = \delta_{ij}$, meaning the $i = 1$ and $i = 2$ terms can be calculated simultaneously. Once again, all terms that arise from anticommuting the fermionic operators will be neglected.

Due to the reasons stated above, the only terms that will actually contribute to the commutator are the combinations of terms with magnon operators of the form $A_q^i(A_{-q}^i)^\dagger$ and $(A_{-q}^i)^\dagger A_q^i$, as only these are nonzero. Note further that since the factor $(-1)^{i+1}$ is equal in the two terms, when multiplying them together they disappear, such that the sign of all expressions for $i = 2$ are the same as those for $i = 1$.

Start by commuting the first term of S with the second and third terms of H_1, giving

$$\sum_{i=1}^{2}\Big[- X_{kq}^i v_{q'i}\big(A_q^i(A_{-q'}^i)^\dagger - (A_{-q'}^i)^\dagger A_q^i\big)c_{k+q,\downarrow}^\dagger c_{k\uparrow} c_{k'+q',\downarrow}^\dagger c_{k'\uparrow} + X_{kq}^i u_{q'i}\big(A_q^i(A_{-q'}^i)^\dagger - (A_{-q'}^i)^\dagger A_q^i\big)c_{k+q,\downarrow}^\dagger c_{k\uparrow} c_{k'+q',\uparrow}^\dagger c_{k'\downarrow}\Big]$$

$$= \delta_{q',-q}\sum_{i=1}^{2}\Big[- X_{kq}^i v_{q'i} c_{k+q,\downarrow}^\dagger c_{k\uparrow} c_{k'+q',\downarrow}^\dagger c_{k'\uparrow} + X_{kq}^i u_{q'i} c_{k+q,\downarrow}^\dagger c_{k\uparrow} c_{k'+q',\uparrow}^\dagger c_{k'\downarrow}\Big] \tag{255}$$

Commute next the second term of S with the first and fourth terms of H_1, giving

$$\sum_{i=1}^{2}\Big[Y_{kq}^i u_{q'i}\big((A_{-q}^i)^\dagger A_{q'}^i - A_{q'}^i(A_{-q}^i)^\dagger\big)c_{k+q,\uparrow}^\dagger c_{k\downarrow} c_{k'+q',\downarrow}^\dagger c_{k'\uparrow} - Y_{kq}^i v_{q'i}\big((A_{-q}^i)^\dagger A_{q'}^i - A_{q'}^i(A_{-q}^i)^\dagger\big)c_{k+q,\uparrow}^\dagger c_{k\downarrow} c_{k'+q',\uparrow}^\dagger c_{k'\downarrow}\Big]$$

$$= \delta_{q',-q}\sum_{i=1}^{2}\Big[- Y_{kq}^i u_{q'i} c_{k+q,\uparrow}^\dagger c_{k\downarrow} c_{k'+q',\downarrow}^\dagger c_{k'\uparrow} + Y_{kq}^i v_{q'i} c_{k+q,\uparrow}^\dagger c_{k\downarrow} c_{k'+q',\uparrow}^\dagger c_{k'\downarrow}\Big] \tag{256}$$

Commute next the third term of S with the first and fourth terms of H_1, giving

$$\sum_{i=1}^{2}\Big[Z_{kq}^i u_{q'i}\big((A_{-q}^i)^\dagger A_{q'}^i - A_{q'}^i(A_{-q}^i)^\dagger\big)c_{k+q,\downarrow}^\dagger c_{k\uparrow} c_{k'+q',\downarrow}^\dagger c_{k'\uparrow} - Z_{kq}^i v_{q'i}\big((A_{-q}^i)^\dagger A_{q'}^i - A_{q'}^i(A_{-q}^i)^\dagger\big)c_{k+q,\downarrow}^\dagger c_{k\uparrow} c_{k'+q',\uparrow}^\dagger c_{k'\downarrow}\Big]$$

$$= \delta_{q',-q}\sum_{i=1}^{2}\Big[- Z_{kq}^i u_{q'i} c_{k+q,\downarrow}^\dagger c_{k\uparrow} c_{k'+q',\downarrow}^\dagger c_{k'\uparrow} + Z_{kq}^i v_{q'i} c_{k+q,\downarrow}^\dagger c_{k\uparrow} c_{k'+q',\uparrow}^\dagger c_{k'\downarrow}\Big] \tag{257}$$

Lastly, commute the fourth term of S with the second and third terms of H_1, giving

$$\sum_{i=1}^{2}\Big[- W_{kq}^i v_{q'i}\big(A_q^i(A_{-q'}^i)^\dagger - (A_{-q'}^i)^\dagger A_q^i\big)c_{k+q,\uparrow}^\dagger c_{k\downarrow} c_{k'+q',\downarrow}^\dagger c_{k'\uparrow} + W_{kq}^i u_{q'i}\big(A_q^i(A_{-q'}^i)^\dagger - (A_{-q'}^i)^\dagger A_q^i\big)c_{k+q,\uparrow}^\dagger c_{k\downarrow} c_{k'+q',\uparrow}^\dagger c_{k'\downarrow}\Big]$$

$$= \delta_{q',-q}\sum_{i=1}^{2}\Big[- W_{kq}^i v_{q'i} c_{k+q,\uparrow}^\dagger c_{k\downarrow} c_{k'+q',\downarrow}^\dagger c_{k'\uparrow} + W_{kq}^i u_{q'i} c_{k+q,\uparrow}^\dagger c_{k\downarrow} c_{k'+q',\uparrow}^\dagger c_{k'\downarrow}\Big]. \tag{258}$$

Gather all the terms, sum over $\vec{k}, \vec{k}', \vec{q}, \vec{q}'$ and multiply by the constants to get

$$\begin{aligned} -\frac{1}{2}[S, H_1] = -\frac{V^2}{2}\sum_{k,k',q,i}\Big[&X_{kq}^i u_{qi} c_{k+q,\downarrow}^\dagger c_{k\uparrow} c_{k'-q,\uparrow}^\dagger c_{k'\downarrow} - Y_{kq}^i u_{qi} c_{k+q,\uparrow}^\dagger c_{k\downarrow} c_{k'-q,\downarrow}^\dagger c_{k'\uparrow} \\ &+ Z_{kq}^i v_{qi} c_{k+q,\downarrow}^\dagger c_{k\uparrow} c_{k'-q,\uparrow}^\dagger c_{k'\downarrow} - W_{kq}^i v_{qi} c_{k+q,\uparrow}^\dagger c_{k\downarrow} c_{k'-q,\downarrow}^\dagger c_{k'\uparrow}\Big] \\ -\frac{V^2}{2}\sum_{k,k',q,i}\Big[&Y_{kq}^i v_{qi} c_{k+q,\uparrow}^\dagger c_{k\downarrow} c_{k'-q,\uparrow}^\dagger c_{k'\downarrow} + W_{kq}^i u_{qi} c_{k+q,\uparrow}^\dagger c_{k\downarrow} c_{k'-q,\uparrow}^\dagger c_{k'\downarrow}\Big] \\ \frac{V^2}{2}\sum_{k,k',q,i}\Big[&Z_{kq}^i u_{qi} c_{k+q,\downarrow}^\dagger c_{k\uparrow} c_{k'-q,\downarrow}^\dagger c_{k'\uparrow} + X_{kq}^i v_{qi} c_{k+q,\downarrow}^\dagger c_{k\uparrow} c_{k'-q,\downarrow}^\dagger c_{k'\uparrow}\Big], \end{aligned} \tag{259}$$

where the result is split into three sums depending on their spin structure.

In terms two and four in the first sum, and term one in the second and third sum, anticommute the two last fermionic operators to the left and redefine the variables by letting $\vec{q} \to -\vec{q}$ and $\vec{k}' \to \vec{k}$. This gives

$$\begin{aligned} -\frac{1}{2}[S, H_1] = -\frac{V^2}{2} \sum_{k,k',q,i} \big(X^i_{kq} u_{qi} + Z^i_{kq} v_{qi} - Y^i_{k',-q} u_{qi} - W_{k',-q} v_{qi}\big) c^\dagger_{k+q,\downarrow} c_{k\uparrow} c^\dagger_{k'-q,\uparrow} c_{k'\downarrow} \\ -\frac{V^2}{2} \sum_{k,k',q,i} \big(Y^i_{k',-q} v_{qi} + W^i_{kq} u_{qi}\big) c^\dagger_{k+q,\uparrow} c_{k\downarrow} c^\dagger_{k'-q,\uparrow} c_{k'\downarrow} \\ +\frac{V^2}{2} \sum_{k,k',q,i} \big(Z_{k',-q} u_{qi} + X^i_{kq} v_{qi}\big) c^\dagger_{k+q,\downarrow} c_{k\uparrow} c^\dagger_{k'-q,\downarrow} c_{k'\uparrow} \end{aligned} \tag{260}$$

Define the three interactions

$$V^{opposite}_{eff} = \frac{V^2}{2} \sum_{i=1}^{2} \big(- Z^i_{kq} v_{qi} - X^i_{kq} u_{qi} + Y^i_{k',-q} u_{qi} + W_{k',-q} v_{qi}\big), \tag{261}$$

$$V^{up}_{eff} = -\frac{V^2}{2} \sum_{i=1}^{2} \big(W^i_{kq} u_{qi} + Y^i_{k',-q} v_{qi}\big), \tag{262}$$

$$V^{down}_{eff} = \frac{V^2}{2} \sum_{i=1}^{2} \big(X^i_{kq} v_{qi} + Z_{k',-q} u_{qi}\big), \tag{263}$$

and anticommute all the creation operators to the front. The full commutator then becomes

$$\begin{aligned} -\frac{1}{2}[S, H_1] = -\sum_{k,k',q,i} \Big[V^{opposite}_{eff} c^\dagger_{k+q,\downarrow} c^\dagger_{k'-q,\uparrow} c_{k\uparrow} c_{k'\downarrow} \\ + V^{up}_{eff} c^\dagger_{k+q,\uparrow} c^\dagger_{k'-q,\uparrow} c_{k\downarrow} c_{k'\downarrow} + V^{down}_{eff} c^\dagger_{k+q,\downarrow} c^\dagger_{k'-q,\downarrow} c_{k\uparrow} c_{k'\uparrow} \Big] \end{aligned} \tag{264}$$

I BCS reduction, two-layer model

This procedure is identical to the one performed in appendix E, as everything is identical up to the summation over i. The procedure starts with considering the effective interactions and inserting the variable changes defined by $\vec{k}' \to -\vec{k}$, requiring $\vec{k} = \vec{k}' - \vec{k}$ and then exchange $\vec{k}$ and $\vec{k}'$.

From equations 109, 110 and 111 the interactions are given by

$$V^{opposite}_{eff} = -\frac{V^2}{2} \sum_{i=1}^{2} \big(Z^i_{kq} v_{qi} + X^i_{kq} u_{qi} - Y^i_{k',-q} u_{qi} - W_{k',-q} v_{qi}\big), \tag{265}$$

$$V^{up}_{eff} = -\frac{V^2}{2} \sum_{i=1}^{2} \big(W^i_{kq} u_{qi} + Y^i_{k',-q} v_{qi}\big), \tag{266}$$

$$V^{down}_{eff} = \frac{V^2}{2} \sum_{i=1}^{2} \big(X^i_{kq} v_{qi} + Z_{k',-q} u_{qi}\big), \tag{267}$$

Inserting the variable redefinitons yields

$$V^{opposite}_{kk'} = -\frac{V^2}{2} \sum_{i=1}^{2} \big(Z^i_{k',k-k'} v_{k-k',i} + X^i_{k',k-k'} u_{k-k',i} - Y^i_{-k',k'-k} u_{k-k',i} - W_{-k',k'-k} v_{k-k',i}\big), \tag{268}$$

$$V^{up}_{kk'} = -\frac{V^2}{2} \sum_{i=1}^{2} \big(W^i_{k',k-k'} u_{k-k',i} + Y^i_{-k',k'-k} v_{k-k',i}\big), \tag{269}$$

$$V_{kk'}^{down} = \frac{V^2}{2}\sum_{i=1}^{2}\left(X_{k',k-k'}^{i}v_{k-k',i} + Z_{-k',k'-k}u_{k-k',i}\right), \tag{270}$$

Rewrite every coefficient as

$$\begin{aligned} X_{kq}^{i} &= \frac{u_{qi}}{\varepsilon_{k\uparrow} - \varepsilon_{k+q,\downarrow} + \omega_{qi}} = \frac{u_{qi}}{\varepsilon_k - m - \varepsilon_{k+q} - m + \omega_{qi}} \\ &= \frac{u_{qi}}{(\varepsilon_k - \varepsilon_{k+q}) + \tilde{\omega}_{qi}^{-}}, \end{aligned} \tag{271}$$

$$\begin{aligned} Y_{kq}^{i} &= \frac{u_{qi}}{\varepsilon_{k\downarrow} - \varepsilon_{k+q,\uparrow} - \omega_{qi}} = \frac{u_{qi}}{\varepsilon_k + m - \varepsilon_{k+q} + m - \omega_{qi}} \\ &= \frac{u_{qi}}{(\varepsilon_k - \varepsilon_{k+q}) - \tilde{\omega}_{qi}^{-}}, \end{aligned} \tag{272}$$

$$\begin{aligned} Z_{kq}^{i} &= \frac{v_{qi}}{\varepsilon_{k+q,\downarrow} - \varepsilon_{k\uparrow} + \omega_{qi}} = \frac{v_{qi}}{\varepsilon_{k+q} + m - \varepsilon_k + m + \omega_{qi}} \\ &= \frac{v_{qi}}{(\varepsilon_{k+q} - \varepsilon_k) + \tilde{\omega}_{qi}^{+}}, \end{aligned} \tag{273}$$

$$\begin{aligned} W_{kq}^{i} &= \frac{v_{qi}}{\varepsilon_{k+q,\uparrow} - \varepsilon_{k\downarrow} - \omega_{qi}} = \frac{v_{qi}}{\varepsilon_{k+q} - m - \varepsilon_k - m - \omega_{qi}} \\ &= \frac{v_{qi}}{(\varepsilon_{k+q} - \varepsilon_k) - \tilde{\omega}_{qi}^{+}}, \end{aligned} \tag{274}$$

where $\varepsilon_k = -t\gamma(\vec{k}) - \mu$, $m = h + SJ_{sd}$ and $\tilde{\omega}_{qi}^{\pm} = \omega_{qi} \pm 2m$.

Starting with the expression for $V_{kk'}^{opposite}$, inserting the reduced coefficients gives

$$\begin{aligned} V_{kk'}^{opposite} = -\frac{V^2}{2}\sum_{i=1}^{2}\Big(&\frac{u_{k-k',i}^2}{(\varepsilon_{k'} - \varepsilon_k) + \tilde{\omega}_{k-k',i}^{-}} - \frac{u_{k-k',i}^2}{(\varepsilon_{k'} - \varepsilon_k) - \tilde{\omega}_{k-k',i}^{-}} \\ &+ \frac{v_{k-k',i}^2}{(\varepsilon_k - \varepsilon_{k'}) + \tilde{\omega}_{k-k',i}^{+}} - \frac{v_{k-k',i}^2}{(\varepsilon_k - \varepsilon_{k'}) - \tilde{\omega}_{k-k',i}^{+}}\Big) \end{aligned}$$

which can be simplified further

$$\begin{aligned} V_{kk'}^{opposite} = -\frac{V^2}{2}\sum_{i=1}^{2}\Big(&\frac{u_{k-k',i}^2\big((\varepsilon_{k'} - \varepsilon_k) - \tilde{\omega}_{k-k',i}^{-} - (\varepsilon_{k'} - \varepsilon_k) - \tilde{\omega}_{k-k',i}^{-}\big)}{(\varepsilon_{k'} - \varepsilon_k)^2 - (\tilde{\omega}_{k-k',i}^{-})^2} \\ &+ \frac{v_{k-k',i}^2\big((\varepsilon_k - \varepsilon_{k'}) - \tilde{\omega}_{k-k',i}^{+} - (\varepsilon_k - \varepsilon_{k'}) - \tilde{\omega}_{k-k',i}^{+}\big)}{(\varepsilon_k - \varepsilon_{k'})^2 - (\tilde{\omega}_{k-k',i}^{+})^2}\Big) \end{aligned}$$

$$V_{kk'}^{opposite} = \sum_{i=1}^{2}\Big(\frac{V^2u_{k-k',i}^2\tilde{\omega}_{k-k',i}^{-}}{(\varepsilon_k - \varepsilon_{k'})^2 - (\tilde{\omega}_{k-k',i}^{-})^2} + \frac{V^2v_{k-k',i}^2\tilde{\omega}_{k-k',i}^{+}}{(\varepsilon_k - \varepsilon_{k'})^2 - (\tilde{\omega}_{k-k',i}^{+})^2}\Big) \tag{275}$$

Performing the same procedure for $V_{kk'}^{up}$, one gets

$$V_{kk'}^{up} = -\frac{V^2}{2}\sum_{i=1}^{2}\Big(\frac{u_{k-k',i}v_{k-k',i}}{(\varepsilon_{k'} - \varepsilon_k) - \tilde{\omega}_{k-k',i}^{-}} - \frac{u_{k-k',i}v_{k-k',i}}{(\varepsilon_{k'} - \varepsilon_k) + \tilde{\omega}_{k-k',i}^{+}}\Big)$$

which can be simplified as

$$V_{kk'}^{up} = -\frac{V^2}{2}\sum_{i=1}^{2}\frac{u_{k-k',i}v_{k-k',i}\big((\varepsilon_{k'} - \varepsilon_k) + \tilde{\omega}_{k-k',i}^{+} - (\varepsilon_{k'} - \varepsilon_k) + \tilde{\omega}_{k-k',i}^{-}\big)}{\big((\varepsilon_{k'} - \varepsilon_k) - \tilde{\omega}_{k-k',i}^{-}\big)\big((\varepsilon_{k'} - \varepsilon_k) + \tilde{\omega}_{k-k',i}^{+}\big)}$$

$$V_{kk'}^{up} = \sum_{i=1}^{2} \frac{V^2 u_{k-k',i} v_{k-k',i} \omega_{k-k',i}}{\tilde{\omega}^+_{k-k',i}\tilde{\omega}^-_{k-k',i} + (\tilde{\omega}^+_{k-k',i} - \tilde{\omega}_{k-k',i})(\varepsilon_k - \varepsilon_{k'}) - (\varepsilon_k - \varepsilon_{k'})^2} \tag{276}$$

Similarly, for $V_{kk'}^{down}$ one gets

$$V_{kk'}^{down} = \frac{V^2}{2} \sum_{i=1}^{2} \Big(\frac{u_{k-k',i} v_{k-k',i}}{(\varepsilon_{k'} - \varepsilon_k) + \tilde{\omega}^-_{k-k',i}} - \frac{u_{k-k',i} v_{k-k',i}}{(\varepsilon_{k'} - \varepsilon_k) - \tilde{\omega}^+_{k-k',i}} \Big)$$

which simplifies to

$$V_{kk'}^{down} = \frac{V^2}{2} \sum_{i=1}^{2} \frac{u_{k-k',i} v_{k-k',i} \big((\varepsilon_{k'} - \varepsilon_k) - \tilde{\omega}^+_{k-k',i} - (\varepsilon_{k'} - \varepsilon_k) - \tilde{\omega}^-_{k-k',i} \big)}{\big((\varepsilon_{k'} - \varepsilon_k) + \tilde{\omega}^-_{k-k',i} \big) \big((\varepsilon_{k'} - \varepsilon_k) - \tilde{\omega}^+_{k-k',i} \big)}$$

$$V_{kk'}^{down} = \sum_{i=1}^{2} \frac{V^2 u_{k-k',i} v_{k-k',i} \omega_{k-k',i}}{\tilde{\omega}^+_{k-k',i}\tilde{\omega}^-_{k-k',i} - (\tilde{\omega}^+_{k-k',i} - \tilde{\omega}_{k-k',i})(\varepsilon_k - \varepsilon_{k'}) - (\varepsilon_k - \varepsilon_{k'})^2} \tag{277}$$

J Calculating the Fermi surface

The Fermi surface is determined by the equation

$$\varepsilon_k = -t\gamma(\vec{k}) - \mu = 0, \tag{278}$$

where

$$\gamma(\vec{k}) = \sum_{\vec{\delta}} e^{i\vec{\delta}\cdot\vec{k}}, \tag{279}$$

and $\vec{\delta}$ is a vector from a lattice site to a neighbouring lattice site. As stated in the model, the lattice is a square 2D lattice with lattice constants $a = 1$. The four lattice vectors are therefore $[1, 0]$, $[-1, 0]$, $[0, 1]$ and $[0, -1]$. Defining

$$\vec{k} = \begin{bmatrix} k_x \\ k_y \end{bmatrix}, \tag{280}$$

the gamma term can be calculated as

$$\begin{aligned} \gamma(\vec{k}) &= e^{ik_x} + e^{-ik_x} + e^{ik_y} + e^{-ik_y} \\ &= 2\cos(k_x) + 2\cos(k_y). \end{aligned} \tag{281}$$

When inserted into equation 278, the equation for the Fermi surface becomes

$$\cos(k_x) + cos(k_y) = -\frac{\mu}{2t} \tag{282}$$

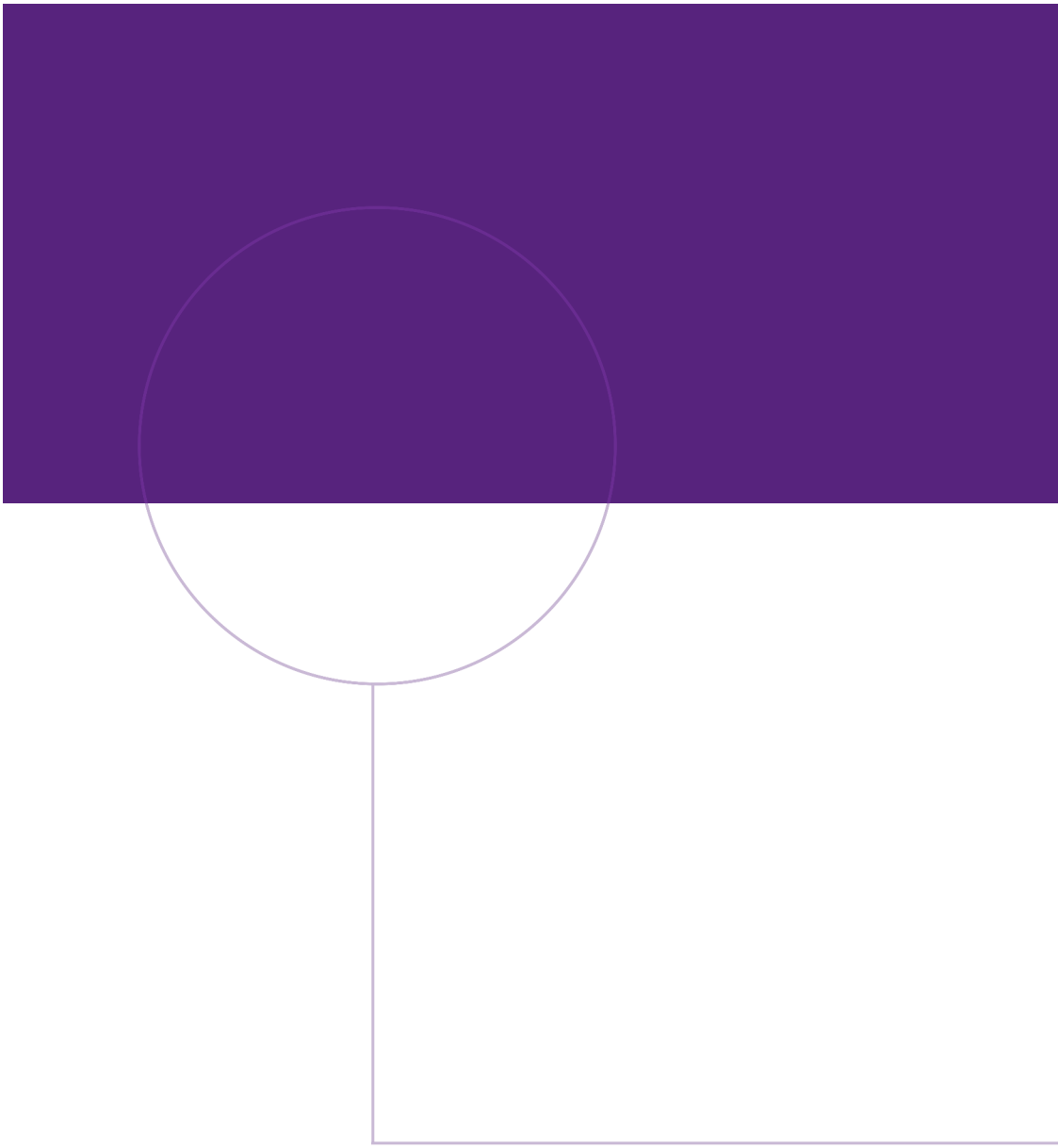

NTNU

Norwegian University of
Science and Technology